SAPIENZA
Università di Roma
Facoltà di Farmacia e Medicina

Ph.D. in
MORPHOGENESIS AND TISSUE ENGINEERING

XXXII Ciclo
(A.A. 2019/2020)

Epigenetic and Transcriptomic profiling of Fibro Adipogenic Progenitors during Duchenne Muscular Dystrophy progression and Histone Deacetylase Inhibitors treatment

Ph.D. Student
Luca Tucciarone

Tutor
Dr Pier Lorenzo Puri
Dr.ssa Silvia Consalvi

Coordinator
Prof. Antonio Musarò

"One day Alice came to a fork in the road and saw a Cheshire cat in a tree.
'Which road do I take?' she asked.
'Where do you want to go?' was his response.
'I don't know,' Alice answered.
'Then,' said the cat, 'it doesn't matter."

— *Lewis Carroll, Alice in Wonderland*

TABLE OF CONTENTS

1 Summary

Duchenne Muscular Dystrophy (DMD) is a severe recessive X-linked disease characterized by the progressive, functional decline of skeletal muscles leading to premature death. There is currently no available therapy for DMD children, thus regenerative pharmacology provides a unique, immediate and suitable resource for the treatment of the present generation of dystrophic patients.
Histone Deacetylase Inhibitors (HDACi) are currently tested in phase II and III clinical trials with Givinostat for the treatment of DMD and Becker Muscular Dystrophy (BMD). Preliminary results demonstrated that HDACi promote muscle regeneration and reduce fibrotic and fatty replacement. However, HDACi beneficial effects are limited to early phases of disease progression, since dystrophic muscles at advanced stages of disease showed resistance to the treatment. Therefore, on-going clinical studies with Givinostat are selectively recruiting ambulant dystrophic boys, in order to enroll a highly chance cohort of responsive patients. This project is thus focused in unraveling what epigenetic mechanisms are modulated by HDACi specifically at early stages of DMD and how the progression of the pathology confer resistance to the treatment. To achieve these goals, we used a Next Generation Sequencing (NGS) approach that takes into account both the epigenetics and transcriptomic changes that happens during HDACi treatment and DMD progression. By performing ChIP-seq for histone acetylation markers (AcH3K9/14 and AcH3K27) we discovered the epigenetic signature that characterize the efficacy of HDACi inhibitors at early but not late stages of DMD: a massive increase of AcH3K9/14 on the promoters of genes related to activation of transcription, cell activation, cell proliferation, cell communication, cell movement and cell survival, as well as a loss of thousands of AcH3K27 peaks outside the promoters; an event we speculate being the termination of putative Fibro-Enhancers.
Our findings also underline the importance of a responsive regenerating environment for TSA activity. Indeed, transplantation of FAPs from unresponsive old dystrophic mice treated with TSA

into young dystrophic muscles recovered several biological features such as cell migration and cell survival. Furthermore, by unveiling the epi-signature of TSA activity and resistance, this study paves the way for the engineering of epigenetic diagnostic tools for assessing the responsiveness to HDACis in candidate DMD boys.

2 Introduction

2.1 The Skeletal Muscle

The Skeletal muscle tissue represents most of our body mass, comprising approximately 40% of total body weight and containing 50–75% of all body proteins. In addition to their major role in locomotion, postural behavior and breathing, the skeletal muscles also function as metabolism regulatory entities serving as glycogen warehouse and site for amino acid catabolism [1]. Myofibers are the histological and functional units of the adult skeletal muscle and stretch along the entire length of its structure. Each single myofiber is surrounded by the sarcolemma (plasma membrane) that interacts with several proteins connected to the internal myofilaments and allows the conservation of the muscle structure. The two most abundant proteins in the skeletal muscle are actin and myosin, which compose approximately 70-80% of muscle total protein content and drive their contraction. There are many other proteins that contribute to the mechanical and physiological proprieties of muscles, such as dystrophin, troponins, titin and nebulin among others. Absence or dysfunction in one of these proteins leads to sarcolemma damage and to a specific disease [1]. At the whole muscle level, the size of a muscle is mostly determined by the number and size of individual myofibers, although pathological infiltration by fat and connective tissue may alter this relationship. Myofibers are multinucleated and post-mitotic. For the most part, each nucleus within a myofiber controls the type of protein synthesized in that specific region of the cell [1]. Individual myofibers are packed tightly together into muscle fascicles with little intervening of connective tissue called the Endomysium. Fascicles are surrounded by the Perimysium and many fascicles align themselves to give rise to the individual body muscles enveloped in the muscle fascia or the Epimysium. Evenly spread running embedded in the connective tissue are nerves and vessels that innervate and supply the myofibers. Thus, the functional properties of skeletal muscle depend on the maintenance of a complex framework of myofibers, motor neurons, blood

vessels and extracellular connective tissue matrix [2] (Figure 1). Due to its mechanical and metabolic tasks it is not surprising that muscle tissue is susceptible to injuries after direct trauma (e.g. intensive physical activities, lacerations) or resulting from indirect causes such as neurological dysfunction or innate genetic defect (e.g. muscular dystrophies). If not repaired, chronic muscle injuries can result in loss of muscle tissue, defects in locomotion, and premature death. To preserve its function, the skeletal musculature shows an impressive regenerative ability in response to injury, activating a finely orchestrated process of cellular responses to environmental cues [2,3].

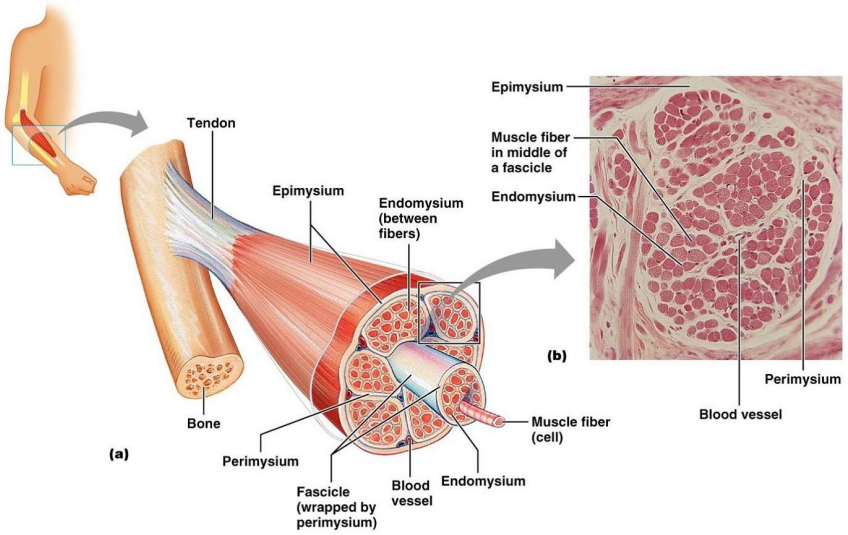

Figure 1: Schematic representation of the skeletal muscle structure. **(a)** Cartoon representing a schematization of the skeletal muscle. **(b)** Histological section of a muscular fascicle. (Pearson education)

2.2 Muscle regeneration

In a complex morphogenetic process during early embryonic development, several myoblasts fuse together to form myotubes. These myotubes serve as a scaffold and eventually increase their size and the number of their nuclei by fusing with additional myoblasts to form multinucleated contractile myofibers. The formation of contractile muscle units from muscle progenitors is a remarkable developmental process that still remains partly understood. Equally remarkable, however, is the regenerative potential of myofibers in the adult muscle tissue. When damaged, muscle tissue is replaced or repaired by the activation and fusion of resident Muscle Adult Stem Cells (MuSCs, or Satellite cells)[2]. Satellite cells are the major contributors to muscle growth, repair, and muscle regeneration [4,5]. Satellite cells are located in a membrane-enclosed niche between the sarcolemma and the basal lamina surrounding the myofibers. Muscle stem cells remain quiescent under normal conditions [6,7], even though cell quiescence is periodically interrupted for the myofibers homeostatic maintenance [8]. Under such conditions, satellite cells likely undergo asymmetric cell divisions that allow the commitment of one daughter cell to the myogenic lineage that is used to reestablish the finite number of nuclei needed for health of the myofiber, and one daughter cell that maintains the satellite cell fate to repopulate the niche [9]. In response to different stimuli, such as exercise, muscle growth or trauma, muscle stem cells can either undergo asymmetric cell division or symmetric cell division giving rise to two daughter cells committed to a massive expansion of the proliferating myogenic progenitor cell pool, and finally differentiate to new myotubes or repair the damaged myofibers [10]. After activation and proliferation, part of the muscle stem cells can return to quiescence and replenish the stem cell pool to prepare for the next regeneration process [11,12].

Whether the muscle injury is inflicted by a direct trauma or innate genetic defects, muscle regeneration is characterized by two phases: a degenerative phase and a regenerative phase [3] (Figure2).

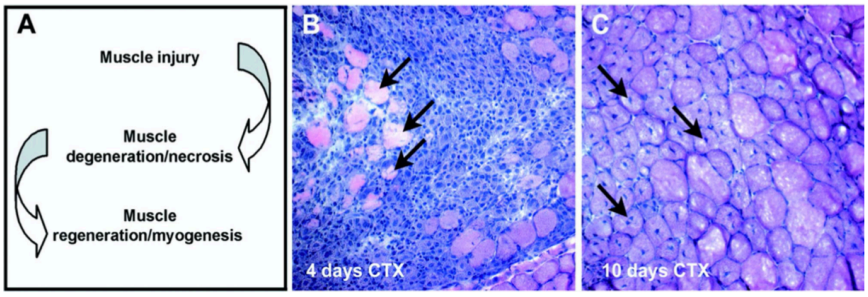

Figure 2: Muscular regeneration process.
(A) Skeletal muscle repair process is characterized by a degenerative phase followed by a regenerative phase. **(B)** Injury by cardiotoxin (CTX) injection results in the rapid necrosis of myofibers, the activation of an inflammatory response and the loss of the muscle architecture. **(C)** Myofiber regeneration is characterized by small and central-nucleated regenerating fibers (arrows) (Charge and Rudnicki 2004).

The initial event of muscle degeneration is the necrosis of myofibers. This event is generally triggered by disruption of the myofiber sarcolemma resulting in increased myofiber permeability which allows cytoplasmic proteins, such as creatine kinase, to leak in the muscular tissue. Disrupted myofibers undergo focal or total autolysis by increased calcium influx after sarcolemmal or sarcoplasmic reticulum damage. The resulting loss of calcium homeostasis and increased calcium-dependent proteolysis, drives tissue degeneration[13]. Calpains, a calcium-activated proteases able to cleave myofibrillar and cytoskeletal proteins are implicated in this process [14]. Infiltration of the damaged muscle by inflammatory cells usually characterizes the early phase of muscle injury and paves the way to muscular regeneration. Factors released by the injured muscle activate resident inflammatory cells that provide the chemotactic signal to circulating inflammatory cells [15]. The first inflammatory cells to invade the injured muscle are the neutrophils. An important increase in their number is observed 1-6 h after muscle damage [16]. Subsequently, about 48 h after injury, macrophages migrate to the damaged area through the bloodstream to remove the cellular debris of impaired myofibers and to activate myogenic cells [17]. Muscle degeneration is followed by a strong regenerative phase. An essential event necessary for muscle repair is the proliferation of myogenic cells. After their expansion,

muscle progenitors differentiate and fuse to damaged fibers for repair, or to one another for new myofiber formation. Newly formed fibers are small, basophilic (because of the high protein synthesis) and express embryonic forms of the Myosin heavy chain (eMHC). When fusion of myogenic cells is completed, the size of the myofibers increases and myonuclei move to the periphery of the fiber. Finally, the repaired muscle tissue is morphologically and functionally equivalent to the un-injured [3].

2.2.1 The Fibro Adipogenic Progenitors

Satellite cells have been shown to be indispensable for adult skeletal muscle repair and regeneration. In the last two decades, other stem/progenitor cell populations resident in the skeletal muscle interstitium have been identified as "collaborators" of satellite cells during regeneration. They also appear to have a key role in replacing skeletal muscle with adipose, fibrous, or bone tissue in pathological conditions. This interstitial cells, can adopt multiple lineages and contribute, either directly or indirectly, to muscle regeneration [18].

Among them, a population of muscle interstitial cells, identified upon expression of PDGFR-α, CD34, and stem cell antigen-1 (Sca1), is endowed with a fibrotic and adipogenic fate that contributes to the regeneration or fibro-adipogenic degeneration of skeletal muscles [19,20]. These cells were originally isolated by two distinct groups in 2010 by fluorescence activated cell sorting (FACS) as CD45-/CD31- (lineage-negative lin-/Sca1+/a7integrin-[19] or as lin-/PDGFRa+/SM/C-2.6- cells [20]. These are two seemingly equivalent cell populations that can collectively be indicated as fibro-adipogenic progenitors (FAPs).

While no myogenic lineage was appreciated in FAPs, these cells could support myogenesis indirectly via functional interactions with myofibers and satellite cells. In resting muscles, FAPs interaction with intact myofibers prevents their conversion into fibro-adipocytes, however, muscle injury stimulates these cells to rapidly proliferate, produce paracrine factors that promote satellite

cell-mediated regeneration [20], and then rapidly disappear [21]. By contrast, in degenerating muscles, such as dystrophic muscles at advanced stages of disease, these cells turn into fibro-adipocytes, which mediate fat deposition and fibrosis, [20,22] thereby disrupting the environment conducive for muscle regeneration. Interestingly, epigenetic reprograming of FAPs by treatment with HDAC inhibitors has been shown to drive them toward a pro-myogenic lineage at the expenses of their native fibro-adipogenic phenotype leading to improved regeneration of dystrophic mice [23] and opening a therapeutic avenue for these progenitors.

The expansion of resident FAPs has been shown to be mediated by the cytokine interleukin 4 (IL-4), produced by eosinophils during the early phases of regeneration [24]. Also, a recent report from Rossi lab has demonstrated that pro-inflammatory cytokines (i.e., tumor necrosis factor, TNF) produced by the first wave of infiltrating macrophages induce apoptosis of FAPs [21]. During chronic injury, such as Muscular Dystrophies, where pro-inflammatory and anti-inflammatory macrophage populations coexist [25], changes in the cytokine milieu (i.e., higher levels of transforming growth factor β1, TGFβ1) prevent the apoptosis of mesenchymal progenitors and induce their differentiation into persistent matrix-producing cells [21]. Furthermore, type 2 cytokine signaling have been shown to activate FAPs for rapid clearance of necrotic debris by phagocytosis, a process that is necessary for timely and complete regeneration of tissues [24].

2.3 Epigenetic control of muscle regeneration

2.3.1 Epigenetics

The first definition of the term 'epigenetics' was: *"changes in phenotype without changes in genotype"*. The term was coined by Waddington in 1942 to explain aspects of development for which there was little mechanistic understanding [26,27]. Almost three-quarters of a century later, we now understand that epigenetic mechanisms can modulate gene expression patterns without altering the underlying DNA sequence but by adapting chromatin, which is the physiological form of our genetic information. Epigenetic mechanisms work in addition to the DNA template to stabilize gene expression programs and thereby direct cell-type identities [28].

Chromatin structure, the way in which DNA is packaged in the eukaryotic cell, has a major impact on transcription levels. In eukaryotes, DNA typically exists as a repeating assortment of nucleosomes, in which 146 bp of DNA are coiled around a histone octamer (consisting of two of each histone proteins H2A, H2B, H3, and H4) [29]. Nucleosomal DNA is generally repressive to transcription; as the nucleosome structure and the DNA-histone interactions make regulatory regions of DNA unavailable for the binding of transcription factors [29]. Histone proteins have tails that project from the nucleosome [30] and many residues in these tails can be post-translationally modified thus to influence chromatin compaction, nucleosome dynamics, and transcription [31]. The definition of chromatin and histone proteins led to the cytological distinction between euchromatin and heterochromatin: cytologically visible ground states of active (euchromatic) and repressed (heterochromatic) chromatin [32]. Chromatin is not an inert structure, but rather an instructive DNA scaffold that can respond to external cues to regulate the many uses of DNA. It is highly dynamic, and creates an accessibility continuum that ranges from closed chromatin to accessible or permissive chromatin (Figure 3) [33].

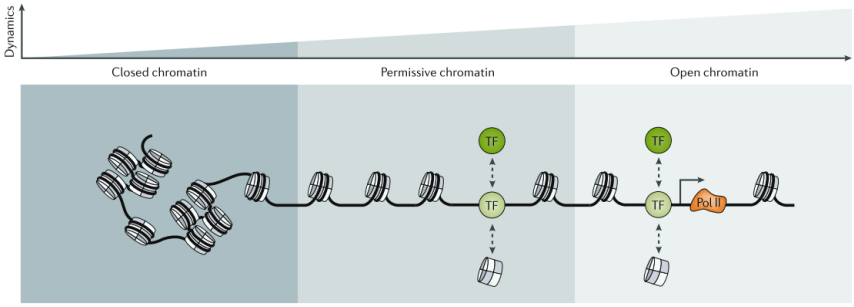

Figure 3: Chromatin dynamics.
Cartoon representing the various degrees of chromatin accessibility. In the figure Pol II (RNA polymerase II); TF, (transcription factors).
(Klemm, Shipony, and Greenleaf 2019).

For instance, the topological organization of nucleosomes across the genome is non uniform: while histones are densely arranged within facultative heterochromatin (chromatin that can be either heterochromatin or euchromatin) and constitutive heterochromatin (chromatin that remains in a condensed state throughout the cell cycle and its further development), they are depleted at regulatory loci (such as promoters or enhancers) [33]. Precisely, facultative hetero-chromatin contains genes that are differentially expressed through development and/or differentiation and then become silenced, while constitutive heterochromatin contains permanently silenced genes in genomic regions such as centromeres and telomeres [34].
Even though the final goal of chromatin relaxation is transcription, protein-coding sequences occupy only a small fraction (<2%) of the mammalian genome, as the rest is occupied with a vast number of cis-regulatory elements (CREs) [35]. CREs are non-coding DNA elements that that govern when, where and how each gene will be expressed. They control transcription by modulating the binding of regulatory proteins, such as transcription factors, to assemble the transcription machinery and initiate transcription by the RNA polymerase II (Pol II) [36]. The most well characterized types of CREs are enhancers and promoters, structural regions of DNA that serve as transcriptional regulators [36,37]. Promoters are specialized DNA sequences surrounding the Transcription Start Site (TSS) of

genes that support the assembly of the transcription machinery and transcription initiation. At ~50 bp surrounding the TSS, the TSS core promoter comprise the binding site for the transcription initiation factor TFIID TBP (TATA-box-Binding Protein) subunit. The proximal part of the promoter, 1-2 kb upstream the TSS, enable the highly regulated transcription of genes by selectively integrating regulatory cues from distal enhancers and their associated regulatory proteins [36]. Enhancers are key gene-regulatory elements that control cell-type-specific spatiotemporal gene expression programs by physical interacting with their related genes, often through long-range chromosomal interactions [37]. In many cases, enhancers can be located at great genomic distances from the target genes they control (in some cases hundreds of kilobases, upstream, downstream or in introns of target genes or unrelated genes) and can bypass more proximally located genes to interact with their target genes [38]. Depending on their post-translational histone modifications, enhancers can be subdivided into various states: neutral (marked by methylation of K4 on histone H3 (H3K4me1)), poised (marked by H3K4me1 and trimethylation of K27 on histone H3 (H3K27me3)) and active (marked by H3K4me1 and acetylation of K27 on histone H3 (H3K27ac)) [39].

2.3.2 Chromatin modifications and modifiers

The assembly and the compaction of chromatin are regulated by multiple mechanisms, including DNA modifications (for example, cytosine methylation) post-translational modifications (PTMs) of histones (for example, phosphorylation, acetylation, methylation and ubiquitylation), the incorporation of histone variants (for example, H2A.Z and H3.3), ATP-dependent chromatin remodeling and non-coding RNA (ncRNA)-mediated pathways [40].

The Post Translational Modifications (PTMs) of the histones tail serve different regulatory purposes in the eukaryotic cells: they may either directly affect chromatin compaction or relaxation, or operate as binding sites for effector proteins (including chromatin-

remodeling complexes), and ultimately influence transcription initiation and/or elongation [40]. The regulation of the PTMs levels is precisely balanced by the Histone Modifying enzymes that can act as "writers" and "erasers". In addition, distinct effector proteins "readers" recognize specific patterns in those modifications [41].
Histone Modifying enzymes are an important class of chromatin-remodeling factors that act by covalently modifying the amino-terminal tail of histones. These include histone acetyltransferases (HATs; also known as lysine acetyltransferases) and histone deacetylases (HDACs; also known as lysine deacetylases); lysine methyltransferases (KMTs) and lysine demethylases (KDMs); and ubiquitylation enzymes (that is, E1, E2 and E3 enzymes) and deubiquitylases (DUBs). These enzymes often exist in multi-subunit complexes and modify specific residues either on the amino-terminal tails or within the globular domains of core histones (H2A, H2B, H3 and H4) [34,40]. Histone modifications exert their effects via two main mechanisms: by either directly influencing the overall structure of the chromatin or by modulating the binding of effector molecules [34]. Histone acetylation and phosphorylation effectively reduce the positive charge of histones, and this has the potential to disrupt electrostatic interactions between histones and DNA, thus promoting chromatin accessibility and facilitating DNA access by protein machineries such as those involved in transcription. In fact, histone acetylations are particularly enriched at enhancers and gene promoters, where they likely facilitate the transcription factor access [42]. Notably, acetylation occurs on numerous histone tail lysines, including H3K9, H3K14, H3K18, H3K27, H4K5, H4K8 and H4K12 [43]. Numerous chromatin-associated factors have been shown to specifically interact with modified histones via many distinct domains that can allow the simultaneous recognition of several modifications and other nucleosomal features. The recruitment of secondary factors on the histone-modified chromatin can result in either propagation of the initial signal or its disruption [34]. For istance, histone acetylated lysines are bound by bromo domains,

which are often found in HATs and in chromatin-remodeling complexes such as the Switch/Sucrose Non Fermentable (SWI/SNF) complex [44]. After histone acetylation, the SWI/SNF remodeling complex can be recruited on acetylated histones, to perpetuate the acetylation signal and "open" the chromatin [45]. Furthermore, histone modifications can positively or negatively affect other modifications by different mechanisms: (I) Competitive antagonism - when multiple histone modifications can happen on the same site(s); (II) Interdependency – when one modification is dependent on the presence of another; (III) Disruption by adjacent modification – when a new modification in the proximity unsettles the stability of another one; (IV) Cooperation – when different histone modifications cooperatively recruit a specific factor [34] (Figure 4).

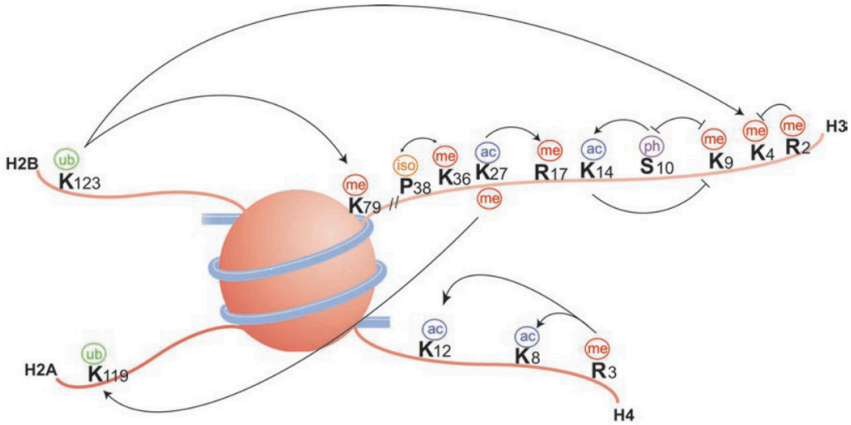

Figure 4: Histone modification crosstalk.
Cartoon summarizing the most common interaction between histone modifications. A positive effect is indicated by an arrowhead and a negative effect is indicated by a flat head. (Bannister and Kouzarides 2011)

Histone methylation mainly occurs on lysines (mono-, di- or tri-methylated; me1, me2 and me3, respectively) and arginines (mono- or di- methylated; me1, me2, respectively) of the histone tail [34]. Unlike other histone modifications, which simply specify active or repressed chromatin states, histone methylations confer active or repressive transcription depending on their positions and methylation states [46]. The enzymes that catalyze the transfer of a methyl group to a lysine are the histone lysine methyltransferase (HKMT). Protein arginine methyltransferases (PRMTs) instead, transfer a methyl group to arginines within a variety of substrates. Methyltransferases and demethylases tend to be relatively specific enzymes for both the histone modification and its specific degree (mono-, di- and/or tri-methyl) [34]. Generally, H3K4, H3K36 and H3K79 methylations are considered to mark active transcription, whereas H3K9, H3K27 and H4K20 methylations are thought to be associated with silenced chromatin states [46].
The same region may have both activating and repressing marks. In fact, bivalent promoters are genetic regions with a co-enrichment of active H3K4me3 and repressive H3K27me3 marks. Those particular types of promoters were shown be responsible for both development of Embryonal Stem Cells (ESCs) [47] and lineage determination into specific cell types [48].
Histone acetylation is the first histone modification discovered [49]. Histone acetyltransferases (HATs) and deacetylases (HDACs) play a critical role in the regulation of gene expression. HATs catalyze the transfer of acetyl groups to lysine residues of histones, resulting in the relaxation of chromosomal DNA [50]. In general, this promotes transcription at the affected chromosomal regions. On the other hand, HDACs eliminate histone acetylation, causing chromosomal DNA condensation and thus, repressing gene expression [51]. HATs, or sometimes referred to as lysine acetyltransferases or KATs, form a superfamily of enzymes that catalyze the transfer of an acetyl group from acetyl CoA to the side-chain amino group of lysine residues on histones, and in some cases other proteins. In doing so, they neutralize the lysine's

positive charge thereby disrupting the stabilizing influence of electrostatic interactions between histones and DNA [52]. Lysine acetylation plays a second role, in addition to changing the charge on the histone tail, it also functions as a binding site for proteins bearing a bromodomain (BD), which tend to be proteins with a pro-transcriptional function. Together, these activities promote a more open, less condensed form of chromatin that is transcriptionally permissive. Indeed, genes whose underlying chromatin is acetylated are more likely to be transcribed [44,52].

There are two major classes of HATs: type-A and type-B. The type-A HATs are diverse family of enzymes that can be classified into three separate groups depending on amino-acid sequence homology and conformational structure: GNAT, MYST and CBP/p300 families [53]. The type-B HATs are highly conserved, predominantly cytoplasmic, and acetylates free histones uncoupled from chromatin. HATs can catalyze the transfer of an acetyl group on a plethora of specific histone acetylation sites in each of the core histones [54], with some differences on the genomic locations. For example, H3K9ac and H3K27ac are highly correlated to the TSS of active genes, whereas H4K12ac and H4K16ac are present at both TSS and along the gene body [42]. H3K14ac has been shown to be required for promoter nucleosome disassembly and nucleosome eviction [55]. H3K9ac has also been recently linked to the recruitment of the super elongation complex (SEC) to promote RNA pol II pause release, and promoting a switch from transcription initiation to elongation [56]. Distal regulatory regions (e.g. enhancers) are also correlated with hyperacetylation of H3K27 [57] (a classical mark of active enhancers) and localization of the HAT, i.e. p300, in combination with mono-methylation of H3K4 [57,58]. Recently, also H3K16ac and the acetylation of globular domain residues H3K122 and H3K64 have also been associated with enhancers, which often lack H3K27ac [59,60].

Moving forward to the HDACs, there are currently 18 known human HDACs that are separated into four classes based on sequence homology to yeast counterparts [29]. There are two main

HDAC protein families: the classical HDAC family and the recently discovered SIR2 family (NAD+-dependent). The Class I, II, and IV HDACs are zinc-dependent enzymes, while class III HDACs (referred to as sirtuins) require NAD^+ [29]. Class I includes HDAC1, HDAC2, HDAC3, and have resemblance to RPD3 in yeast. HDAC4, HDAC5, HDAC7 and HDAC9 belong to class II and have resemblance to another yeast deacetylase, HDA1 [50]. Class II HDACs are considered to be involved in developmental processes and cellular differentiation due to their specifically restricted expression behavior, unlike those of class I [61]. HDAC6 contains two catalytic sites and is classified as class IIb, whereas HDAC11 has conserved residues in its catalytic center that are shared by both class I and class II deacetylases and is placed in class IV [62] .

2.3.3 The epigenetics of muscle regeneration

Skeletal muscle regeneration is an efficient stem cell-based repair system that ensures healthy musculature. Dynamic change of epigenetic landscape to control DNA accessibility and expression is a critical component during myogenesis for the effective repair of damaged muscle. PTMs, nucleosome repositioning, and DNA methylation are events which collectively allow the control of changes in transcription networks during transitions of MuSCs from a dormant quiescent state toward terminal differentiation [9]. Each of the myogenic cell fates (satellite cells, myogenic progenitor cell, myofibers) associated with muscle regeneration is characterized by a distinct gene expression program [9]. In the uncommitted satellite cell, the paired-box gene, Pax7, plays an essential role in maintaining the stem cell identity of this population [9]. Upon activation, satellite cells can become committed to the myogenic lineage by expressing the family of muscle regulatory factors (MRFs) such as the Myoblast Determination protein 1 (MyoD), Myogenic factor 5 (Myf5) and 6 (Myf6 or Mrf4) and Myogenin (Myog). MyoD is the master regulator of the skeletal muscle gene expression program and follows every stage

of myogenesis, from the expansion of myoblasts (when it couples with Myf5) to terminal differentiation (when is expressed alongside Myogenin, Figure 5) [63].

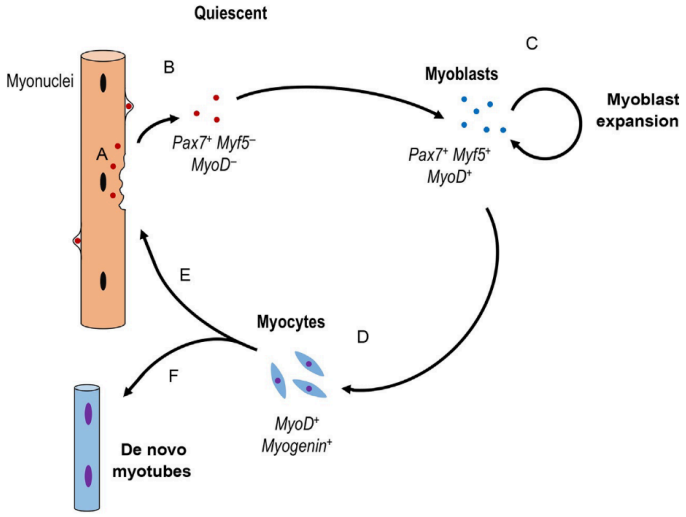

Figure 5: Transcriptional signature of muscular regeneration.
After muscle damage, (A) quiescent satellite cells (Pax7+/Myf5-/MyoD-) localize to the site of injury, (B) where they activate and enter the myogenic differentiation. (C) Activated satellite cells become proliferating myoblasts and expand the pool of muscle progenitors (Pax7+/Myf5+/MyoD+). (D) Myoblasts become myocytes committed toward terminal differentiation (MyoD+/Myogenin+) and either (E) repair damaged myofibers or (F) create new ones. (Robinson and Dilworth 2018)

The muscle regulatory factors (MyoD, Myf5, Mrf4 and Myogenin), depend upon accessory transcription factors such as myocyte enhancer factor 2 (MEF2) [9] and Sineoculis homeobox homolog (SIX) families [64]. In healthy muscles, satellite cells are maintained in a quiescent state by repressive PTMs on myogenic genes. In this context, PRC2 marks genes required for proliferation and differentiation with H3K27me3 [65,66], and the Suv4-20h1 methyltransferase closes the promoter of MyoD with H4K20me2 [67]. After traumatic stress, muscle regeneration relies on satellite cell myogenesis for the formation of new myofibers under the

control of myogenic regulatory program and mitogenic factors released by inflammatory cells (i.e. macrophages), FAPs and damaged myofibers. For instance, several lines of evidence indicate that regeneration-activated p38 signaling targets multiple components of the myogenic components that are assembled on the chromatin of muscle genes in response to locally released regeneration cues. Activation of the quiescent satellite cell in response to extrinsic cues occurs through a series of gene activations that necessitate changes in histone methylation and acetylation. The arginine methyltransferase CARM1 methylates Pax7 during asymmetric satellite cell division [68] targeting Pax7 to activate the Ash2L/MLL2 complex [69] that mediated the permissive H3K4me3 on genes involved in establishing the muscle cell fate, such as Myf5 [68,69]. In this phase also MyoD gets expressed but the changes in methylation are not well established, though it is clear that a loss of the repressive H4K20me2 mark is observed through a mechanism that remains to be determined [67]. It is noteworthy to mention that in asymmetric division, specific activation of Myf5 only occurs in the daughter cell that will become activated, whereas the other daughter cell that will return to a quiescent state will not activate Myf5 [9]. At this stage, Myoblasts are allowed to expand because the promoter of Myogenin is tightly methylated in both H3K27me3 [66] (by PRC2/Ezh2 associated with the YY1 transcription factor) and H3K9me3 [70] (by Suv39h1/KMT1A).
In particular, the p38γ MAPK signaling cascade is responsible for the phosphorylation of MyoD on Ser199 and Ser200 that in turns recruit of the Suv39h1/KMT1A methyltransferase on the Myogenin promoter [71]. This is a key regulatory step as Myogenin expression represents a point of no return for progenitors to commit to muscle differentiation [72].
The ability of myogenic progenitor cells to undergo terminal differentiation requires a coordinated series of changes in gene expression that allow cell cycle exit in concert with the activation of muscle-specific genes for the formation of functional multinucleated myofibers. In this context, the modulation of

histone acetylation and methylation are tightly linked with MRF family members, such as MyoD. For example, MyoD and MEF2 act cooperatively to regulate the expression of skeletal muscle-specific genes [73] and non-coding RNAs involved in the activation of the myogenic program [74]. These two classes of transcription factors associate with HATs and HDACs to control the activation and repression, respectively, of the muscle differentiation program [9]. HDACs are very important in controlling myogenic differentiation. In undifferentiated myoblasts, association of MyoD and MEF2 factors mediates HDAC recruitment to the chromatin of target genes and prevents hyperacetylation and activation of muscle gene expression [9]. Interestingly, while class I HDACs (HDAC1 and HDAC2) show constitutive nuclear localization and preferential association with MyoD [75,76], class II HDAC members, HDAC4 and 5, shuttle between the nucleus and the cytoplasm and are dedicated repressors of MEF2-dependent transcription [77]. Upon differentiation, dislodgment of HDACs from the chromatin of target genes correlates with the hyperacetylation at muscle genes loci and activation of transcription [78]. Moreover, acetylation at the promoter of MyoD and MEF2 factors contribute to stimulate transcription of target genes [79–81]. During terminal differentiation, while the UTX histone demethylase actively removes H3K27me2/3 histone marks [82], PRC2/Ezh2 is downregulated , allowing a loss of repression on myogenic genes to pave the way to terminal differentiation [65]. The UTX-mediated specific removal of H3K27me3 repression marks is mediated by the transcription factor SIX4 [83] and directly facilitated by the histone chaperone spt-6 cooperative interactions [84]. On the other hand, PRC2 is involved in the H3K27 tri-methylation of genes involved in the cell cycle, such as cyclin D1 [85]. At this stage, MyoD expression is increased thanks to the p300-mediated H3K18ac, H3K9ac and H3K27Ac on its enhancer [86] . When unleashed, MyoD can partner with other MRFs, histone modifying enzymes or chromatin remodelers to promote terminal differentiation [9]. MyoD and MEF2 can guide the histone demethylase LSD1 to muscle-specific genes for removal of

H3K9me3 mark [87], thus promoting H3K9 acetylation [66]. In addition, MyoD binding may allow for opening of chromatin structure through specific histone acetyltransferase recruitment. In fact, although a global decrease in acetylation is observed in terminal differentiation of myoblasts [88], there is an overall increase in H4 acetylation at sites that were also bound by MyoD [89]. Precisely, p300, pCAF and MyoD actively form complexes on promoters of MyoD target genes [90] for the recruitment of transcriptional coactivators [91]. In myogenic differentiation, SWI/SNF complexes containing either Brg1 or Brm ATPase subunits have been shown to regulate genes for terminal differentiation (i.e Myogenin and MyHC) and cell cycle arrest, such as Ccnd1 [92]. The targeting of SWI/SNF to the myogenic loci is mediated through a direct interaction between MyoD and the BAF60c subunit of the complex [93]. When committed toward terminal differentiation, activation of the p38α/β kinases phosphorylates BAF60c, that gets incorporated into the Brg1–SWI/SNF complex at the MyoD-directed muscle-specific gene promoter [93]. Finally, macrophage infiltration and damaged myofibers secrete cytokines, such as the tumor necrosis factor alpha (TNF-α) that activates the p38α signaling cascade [9]. The signaling, culminates with the phosphorylation of both MEF2D and EZH2/PRC2. MEF2D recruits Ash2L/MLL2 methyltransferase complex on the promoters of myogenic differentiation genes such as Myogenin, to deposit transcriptionally permissive H3K4me3 [94] . On the other hand phosphorylated EZH2/PRC2 catalyzes the formation of repressive chromatin on Pax7 promoter by depositing H3K27me3 [95].

2.4 Epigenetic correction of Duchenne Muscular Dystrophy progression

The understanding of the epigenetics in muscle regeneration led to new therapeutic approaches that directly target epigenetic regulating mechanisms to promote efficient muscle regeneration in patients affected by muscle-wasting diseases, such as Muscular Dystrophies (MD).

2.4.1 Duchenne Muscular dystrophy

Muscular dystrophies are inherited myogenic disorders characterized by progressive muscle wasting and weakness of variable distribution and severity. There are several types of muscular dystrophies, classified based on predominant muscle weakness: Duchenne (DMD) and Becker (BMD); Emery-Dreifuss; facioscapulo-humeral; oculopharyngeal; limb-girdle which is the most heterogeneous group.
DMD is a severe X-linked recessive condition that affects ~1 in 5,000 newborn boys [96]. DMD is a progressive genetic disorder caused by mutations in the *dystrophin* gene that result in the absence of functional protein [97]. First symptoms become apparent at the age of 2–3 years. The gradual loss of muscle tissue and function leads to wheelchair dependency at approximately the age of 12 years, the need for assisted ventilation at approximately the age of 20 years and premature death, usually in the third or fourth decade of life [98]. Dystrophin is an unusually large structural protein that connects, via the dystrophin-associated protein complex (DAPC), the cytoskeleton of myofibers to the extracellular matrix, thereby acting as an important stabilizer of myofibers during movement [98]. The DAPC links the actin cytoskeleton to the extracellular matrix and has an essential role in stabilizing the sarcolemma during repeated cycles of contraction [99]. In the absence of dystrophin, the structural and functional integrity of the DAPC is compromised and the myofibers become damaged during contraction. The chronic nature of this damage results in

inflammation, which in turn inhibits muscle fibre regeneration. Even if at the first stages of DMD the regeneration is able to counterbalance muscular degeneration, ultimately, these continuous damages lead to the replacement of muscle by fibrotic scars and adipose tissue deposition [96]. This 'restriction point' in the progression of DMD is due to alterations in the interactions between different cell types that contribute to promote regeneration, eventually culminating with a switch of muscle repair toward fibrotic and fat deposition. In particular, studies in the last decade have revealed the importance of changes in the identity and functional properties of the cellular components of MuSCs niche. For instance, the interactions between inflammatory cells (e.g. macrophages), interstitial 'supportive' cells (e.g. FAPs) and MuSCs appear a key determinant to drive the skeletal muscle toward a regenerative or degenerative process [100]. This notion has inspired a number of current pharmacological strategies aimed at targeting these cells and the functional networks they establish as an alternative to gene replacement and cell-based strategies [21,101] . Moreover, in contrast with the other strategies, regenerative pharmacology is potentially applicable to any genetic sub-type of DMD and other Muscular Dystrophies.

2.4.2 Therapies for DMD

Although there is currently no available cure for DMD, different therapeutic strategies are being developed to either restore functional Dystrophin or enhance muscle function in a Dystrophin independent manner [96]. However, DMD poses a vast plethora of challenges to therapies. First, the target tissue, skeletal muscle, is highly abundant and makes up 30–40% of our body mass. The human body has > 500 different skeletal muscles, almost all of which to some extent are affected by DMD. Because DMD pathology is caused by the lack of functional dystrophin, restoring the function or expression of dystrophin is an obvious therapeutic approach. The strategies developed by this therapeutic approach

are the Gene Therapy and the Stem Cell Therapy in which the former makes an effort to re-establish the expression of Dystrophin, while the latter involves the transplantation of functional dystrophin expressing MuSCs in dystrophic muscles [96].
A particular efficient gene therapy is the exon skipping. The exon-skipping approach is based on the fact that most patients with DMD could in theory produce a BMD-like dystrophin if the reading frame could be corrected. Exon skipping uses antisense oligonucleotides which bind to a specific sequence in the target exon in the pre-mRNA dystrophin transcript, inducing skipping of the target exon during the splicing, which restores the reading frame and enables the production of a partially functional dystrophin. This approach is mutation specific. However, most patients with DMD have a deletion of one or more exons, and these deletions are typically clustered in exons 43–55. Thus, skipping of particular exons is applicable to larger subgroups of patients [102].
The third alternative to the gene therapy and cell stem cell therapy is the pharmacological therapy. This approach consists in different strategies that aim to counteract DMD progression by improving muscle function and muscle regeneration. Among those pharmacological interventions, the HDACi aim to slow down DMD progression by targeting key events downstream of the genetic defect. Mounting evidences in the last ten years have demonstrated the beneficial effect of HDACis in counteracting Muscular Dystrophies [23,101,103–106].
In particular Givinostat is currently undergoing in clinical trials of phase II/III and III in ambulant patients affected by DMD (link here[1] and here[2]), and a phase II clinical trial on patients affected by BMD (link here[3]), based on the encouraging pre-clinical data generated in the mouse model of DMD – the mdx mice [104,105]. In particular, Consalvi and collogues in 2013 demonstrated the ability

[1] https://clinicaltrials.gov/ct2/show/NCT03373968
[2] https://clinicaltrials.gov/ct2/show/NCT02851797
[3] https://clinicaltrials.gov/ct2/show/NCT03238235

of Givinostat to enhance muscle performance, muscle regeneration and to reduce inflammation and fibrosis in the mdx mice [105]

2.4.3 Epigenetic treatment for DMD: HDACis

Large amount of work illustrated the fundamental role of HDACs and HATs in regulating muscle development [9,107] in physiological and pathological conditions. Despite the general assumption that HDAC inhibition would indiscriminately cause a global hyperacetylation in all organs and tissues, several studies revealed a surprising selective effect of HDACi on pluripotent cells (both embryonic stem cells and adult, resident stem cells) able to self-renew and proliferate [108]. Studies performed in mdx mice indicate that dystrophin deficiency leads to deregulated HDAC activity, which in turn perturbs downstream networks. As mentioned in the previous paragraphs, the absence of dystrophin delocalizes the DAPC and downregulates NO synthase (nNOS), which inhibits HDAC2 activity by S-nytrosylation. This is consistent with a global deficiency of NO observed in dystrophic muscles [109]. Deficient S-nitrosylation of HDAC2 leads to constitutive inhibition of target genes [110]. It is likely that DAPC-regulated NO signaling to HDAC2 mediates transcriptional adaptation to mechanical cues, such as those derived from myofiber contraction. One key gene controlled by HDAC2 in muscle cells is Follistatin [104], the endogenous antagonist of the most potent inhibitor of skeletal myogenesis: Myostatin [111]. An unbalanced Follistatin/Myostatin activity, caused by deregulated HDAC2 function contributes to DMD pathogenesis [110]. Consequently, it is possible that HDAC-mediated induction of Follistatin transcription in FAPs [101] is important to maintain proper myofiber structure post-contraction and to increase muscle mass. Furthermore, reduced HDAC2 nytrosylation translates in a decreased expression of several “myomiRs” (miRNAs related to myogenesis) such as miR1 and miR29 in mdx muscles [112]. Indeed, restoring the NO signaling to HDAC2 in mdx mice, by exon

skipping, led to de-repression of these myomiRs. Importantly, several networks controlled by the both identified myomiRs, explain some of the DMD pathogenetic traits, for example: miR-1 explains the redox state of the cell and miR-29 the fibrotic process [112]. Recent evidence demonstrates a reciprocal control between myomiRs and MyoD/MEF2-responsive promoters [74,113], which in turn, are typically regulated by HDACs. MiR-1 and miR-133, two myomiRs clustered on the same chromosomal locus, have specific roles in modulating skeletal muscle proliferation and differentiation [113]: miR-133 enhances myoblast proliferation by repressing serum response factor (SRF) while miR-1 is induced during myogenic differentiation and downregulates HDAC4, leading to activation of MEF2-induced gene transcription. HDACi in this context are predicted to promote the expression of myomiR in myoblasts. Collectively, these data demonstrate that de-regulated DAPC/NO signaling to HDAC2 in dystrophic muscles is an important epigenetic contributor to DMD pathogenesis, as it controls the expression of coding and non-coding genes involved in muscle regeneration, fibrosis and oxidative stress.

HDACi are compounds that alter the epigenetic markers of histones, thereby influencing the expression of multiple genes. Clinically relevant HDAC inhibitors are classified by their chemical structure: hydroxamic acids, short chain fatty acids, cyclic peptides, and benzamides. Among those, hydroxamic acids are very interesting as their effectiveness lies within micro to nano-molar concentration range [62,114]. The most relevant hydroxamic acids we can find Vorinostat (suberoylanilide hydroxamic acid, SAHA), Trichostatin A (TSA) and Givinostat (ITF2357). Interestingly, TSA was the first natural hydroxamate discovered to inhibit HDACs [115]. The mechanism underlying the function of individual HDAC inhibitors remains largely unknown [116]. Several identified co-crystal structures about HDAC8 suggests that hydroxamates (such as TSA or Vorinostat) act via a zinc chelation process happening directly into the catalytic pocket of the protein. Despite the limited understanding of the mechanisms behind

HDAC inhibitor action, there is rising experimental and clinical evidence indicating that these epigenetic drugs not only can be effective in the treatment of malignancies, inflammatory diseases and degenerative disorders, but also in the treatment of genetic diseases, such as Muscular Dystrophies. In principle, the rationale for using HDACi as a treatment for DMD was provided by the finding that dystrophic muscles display an aberrant, constitutive activation of HDAC2, as a consequence of reduced nitric oxide (NO)-mediated inhibitory S-nitrosylation of HDAC2 in myofibers [110]. Indeed, direct inhibition of HDAC2 by HDACi, or inactivation by either nitric oxide donors or by reconstitution of the dystrophin-NO signaling leads to de-repression of Follistatin, which mediates the ability of HDACi and NO signaling to stimulate myogenesis *in vitro* [103,110,117] and counters muscle degeneration in mdx mice by impairing fibrotic and adipogenic deposition and enhancing both myofiber size and muscle regeneration [104]. Previous studies from Puri's lab described the relative ability of different HDACi to counter DMD progression. Minetti et al. showed that exposure to distinct HDACi—trichostatin A (TSA), valproic acid (VPA) and phenylbutyrate— effectively countered disease progression [104]. These compounds are general inhibitors of HDACs (pan-HDACi) that enhanced Satellite cells ability to form larger myotubes *in vitro* [103,117]. The comparable efficacy of MS275, which selectively inhibits class I HDACs and pan-HDACi suggests that inhibition of class I HDACs is sufficient to exert most of the beneficial effects observed in HDACi-treated mdx mice [104]. Interestingly, the extent by which HDACi ameliorates the mdx phenotype varies significantly among these compounds, with HDACis (and in particular TSA) being the most effective drug at defined concentrations (TSA 0.6 mg/kg, delivered by daily intra-peritoneal injection) [104]. Recent studies revealed complex epigenetic networks targeted by TSA in MuSCs and FAPs [23,112]. In particular, Saccone et al. identified an HDAC-regulated network that promotes a phenotypical switch in dystrophic FAPs. HDACis are able to dramatically impair FAP fibro-adipogenic potential and activate a

latent pro-myogenic phenotype that supports MuSC-mediated muscle regeneration, by upregulating specific myomiRs that target a key chromatin remodeler: the SWI/SNF. Treatment with HDACi promotes the expression of two core components of the myogenic transcriptional machinery, MyoD and BAF60c [93] and upregulates three myogenic microRNA involved into muscle differentiation (myomiRs; miR-1.2, miR-133 and miR-206) in FAPs. The HDACi induced myomiRs in turn, promote the incorporation of BAF60c into the SWI/SNF chromatin-remodeling complex by inhibiting two alternative BAF60 variants - BAF60a and b - that would otherwise promote the activation of the fibro-adipogenic program [23]. In this way HDACis mediate a therapeutic switch of FAP phenotype from fibro-adipogenic to pro-myogenic. Interestingly, FAPs from dystrophic muscles at advanced stage of the disease become resistant to the beneficial effects of HDACi, as no histological nor phenotypical effect have been observed after treatment [101]. Previous studies have already showed a stage-dependent effect of HDACi in muscle cells in proliferating myoblasts and muscle progenitors during somitogenesis and adult muscle regeneration [103,117,118]. Microarray analysis indicated that TSA significantly perturbs the gene expression profile in human myoblasts but not in terminally differentiated myotubes. The large majority of the genes upregulated by TSA in myoblasts are involved in the myogenic differentiation program indicating that HDACi anticipate the expression of genes that are normally induced during differentiation [118]. More recent genome-wide studies of chromatin accessibility also showed that at early stages of the disease, HDACi promote an extensive chromatin remodeling, which was not observed at late stage of DMD [23].
Taken together, these findings indicate that HDACIs are able to effectively counteract DMD progression. Unlike with steroids, which currently are used as palliative treatment in muscular dystrophies, the molecular rationale and the epigenetic basis of the beneficial effect of HDACi are being revealed. In particular, HDACi reprogram FAP phenotype by modulating their

epigenome, but a permissive epigenetic landscape is needed. In this context, DMD onset offers such landscape but during DMD ageing, it changes and FAPs become resistant to HDACi intervention. Understanding the molecular basis of such resistance could reveal novel targets for interventions aimed at restoring the ability of FAPs to support muscle regeneration rather than fibrosis and fat infiltration, in a larger population of dystrophic patients.

3 Aims

This project aims to unravel the epigenetic and transcriptomic mechanisms responsible of the stage-specific efficacy of HDACis in modulating dystrophic FAPs phenotype and function during DMD progression.

Previous studies from Puri's lab reported the ability of HDACi to ameliorate the pathology of Muscular Dystrophies by promoting functional and morphological recovery of dystrophic muscles at the expense of fat and fibrosis deposition [104]. Recently, the cellular effectors responsible of such beneficial effect have been elucidated. In the orchestra of different cellular populations involved in muscle regeneration, the HDACi potentiate the crosstalk between the FAPs and MuSCs [101]. Precisely, HDACis are able to reprogram FAPs phenotype and activate a latent myogenic program that is able to support MuSCs-mediated muscular regeneration at the expenses of their native fibro-adipogenic phenotype [23].

The HDACi Givinostat has recently entered into phase II/III clinical trials for BMD and DMD on the basis of pre-clinical studies on mdx mice [105], the murine model of DMD. Current clinical studies confirmed the ability of Givinostat to counteract DMD progression by enhancing endogenous regeneration, increasing myofiber size, while preventing fibrotic scars and fat deposition.

However, our previous data showed that HDACi beneficial effects are limited to early phases of disease progression, since at advanced stages of disease dystrophic muscles and FAPs become resistant to the treatment [101]. Indeed, current clinical trials with Givinostat are selectively recruiting ambulant young dystrophic boys, in order to enroll a highly chance cohort of responsive patients.

Therefore, the main challenge of this project is to elucidate the epigenetic mechanisms specifically modulated by HDACis at early

and late stages of DMD and understand their translation into FAP phenotypical changes.

Here are reported the specific aims with the chosen experimental approaches:

- Aim 1: Epigenetic and Transcriptomic profiling of FAPs during DMD progression and HDACi treatment.

We used an NGS approach to draw the profile of the epigenetic (ChIP-seq for AcH3K9/14 and AcH3K27) and transcriptomic landscape of FAPs during the progression of the pathology and TSA treatment.

- Aim 2: Revealing the DMD-stage specific Epigenetic signature of HDACi.

With a Bioinformatic approach we were able to dissect the epigenome of FAPs and map the specific and overlapping differences between the treatment of TSA at early and late stages of DMD.

- Aim 3: Translate the epi-signature that characterize the efficacy and resistance to HDACi-induced beneficial effects into FAPs phenotypical changes.

With a multidisciplinary analysis that embraces *in silico* and *in vivo* experiments, we were able to connect the HDACi epigenetic signature to the modulation of key biological FAP functions relevant for muscular regeneration.

4 Results

4.1 TSA drives different patterns of histone acetylation profiles in FAPs depending on DMD progression.

Recent studies conducted in the murine model of DMD, the mdx mice, have revealed the crucial role of FAPs in muscle regeneration [21,24] and identified them as the key target population mediating the HDACi beneficial effects [101]. The epigenetic modifications triggered by HDACi (precisely TSA) in dystrophic FAPs converge in a phenotypical switch towards the suppression of their native fibro-adipogenic phenotype and the activation of a latent myogenic phenotype that supports MuSC-mediated muscular regeneration [23].

However, it has also been shown that the ability of TSA to reprogram FAP phenotype is restricted to the early stages of DMD (1.5-month-old mdx mice), since at late stages (12-month-old mdx mice) dystrophic FAPs seem resistant to the treatment, and contribute to muscle wasting by depositing fibrotic and adipogenic scars [101].

In order to gain further insights on HDACi epigenetic activity, we adopted a genome-wide approach to evaluate the histone acetylation profile of FAPs isolated from mdx mice at early and late stages of the pathology (hereafter referred as young and old, respectively) treated with TSA for 15 days (TSA) or its vehicle of control (CTR). In detail, we performed ChIP-seq for acetylation of histone 3 at lysine 9/14 (AcH3K9/14) and lysine 27 (AcH3K27) coupled with RNA-seq: two histone marks respectively enriched in promoter and enhancer regions and involved in gene expression activation (Figure 6).

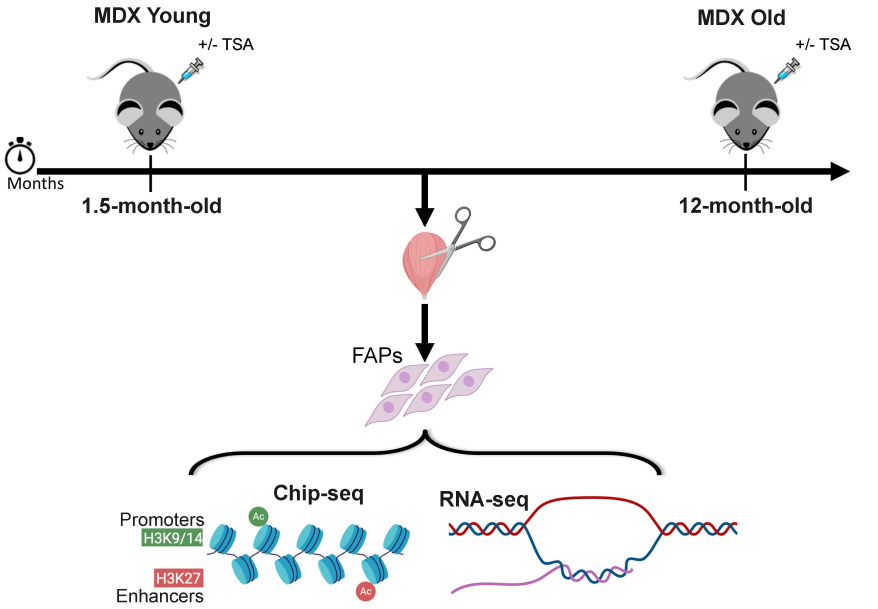

Figure 6: NGS approach to study FAP epigenetic landscape and transcriptomic modulation during DMD progression and HDACi treatment.
Cartoon describing the Next Generation Sequencing approach used. In detail: MDX mice at 1.5 Months (Young) and 12 Months (Old) of age were treated with TSA or its vehicle of control for 15 days. At the end of the treatment FAPs were isolated by FACS from hindlimb muscles to perform ChIP- and RNA-seq.

We started our ChIP-seq analysis by looking at the overall genomic distribution of the acetylation on H3K9/14 and H3K27. As expected, AcH3K9/14 is prevalently located within the promoter boundaries while AcH3K27 is mainly associated outside it (Figure 7A). Our analysis of the ChIP-seq experiment revealed that FAPs acquire a completely different pattern of chromatin acetylation along DMD progression and HDACi treatment (Figure 7B). In Young FAPs, TSA increases AcH3K9/14, with a more pronounced effect on promoter regions and unexpectedly drops AcH3K27 outside the promoter boundaries. During the progression of the pathology, Old FAPs obtain a diffuse enrichment of H3K9/14 acetylation beside a strong decrease of AcH3K27. In this

altered epigenetic context, TSA loses the ability to substantially increase AcH3K9/14, and globally spreads the acetylation of H3K27 (Figure 7B).

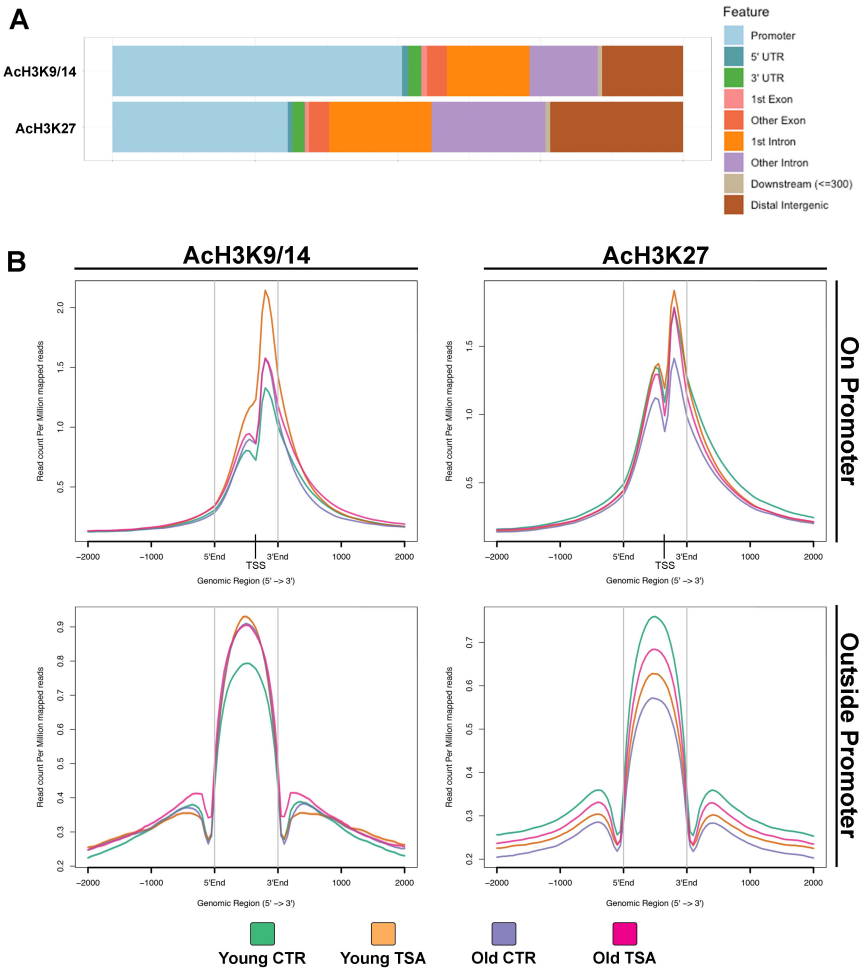

Figure 7: TSA treatment hyperacetylation presents a differential specificity during DMD progression
A) Genomic distribution of the ChIP-seq signal for AcH3 and AcH3K27. The colorimetric legend is on the left. **B)** Visualization of ChIP-seq patterns by NGS plot for both AcH3k9/14 and AcH3k27 on promoters (upper panels) and outside promoters (lower panels). Promoters defined as -1500/+500 bp from the Transcription Start Site (TSS).

4.2 Defining the HDACi stage-dependent episignature.

In order to better understand how DMD progression and TSA alter the epigenetic landscape of FAPs, we developed a custom pipeline of differential peak calling in the three main comparison of interest (Young CTR vs Young TSA, Young CTR vs Old CTR and Old CTR vs Old TSA). Significant differential peaks between samples were extrapolated and characterized based on acetylation levels (Hyper Acetylation or De Novo Acetylation) and genomic distribution (in and out the promoter) (Figure 8A).
According to the NGS plots in figure 7B, we discovered 12553 loci with increased acetylation in H3K9/14 in Young FAPs exposed to TSA, 63% of which are hyper-acetylated and mostly located on promoters (see first comparison Young CTR vs Young TSA). Furthermore, at this stage TSA drops 3198 peaks of acetylation for AcH3K27, more than 70% of which are outside promoters and have lost the acetylation. This result suggests that in young responsive FAPs, TSA substantially promotes hyper-acetylation on gene promoters and indirectly affects enhancer activation.
During the progression of DMD we observed a general increase of AcH3K9/14 (4621 differential loci) and a dramatic loss of acetylation in H3K27 (12631 differential loci) without particular enrichment for either kind of acetylation or genomic distribution (see second comparison Young CTR vs Old CTR). Our speculation is that these loci simultaneously acquire H3K27me3 along DMD progression.
In this altered epigenetic landscape, TSA almost completely loses the ability to hyper-acetylate H3K9/14 on gene promoters (only 2410 loci increase acetylation in old FAPs compared to 12553 in young FAPs after TSA treatment) but gains the novel ability to globally increase the acetylation on H3K27 on 4473 loci (see third comparison Old CTR vs Old TSA).

All together our differential analysis shows a completely different epi-signature of HDACi activity at different stages of DMD pathology.
We then sought to understand whether the differential regions of acetylation presented binding sites for different DNA-binding factors, such as Transcription Factors (TFs). In figure 8B are shown the most abundant binding sites for families of TFs found on the peaks that are lost (Lost) or gained (Gained) by TSA at Young (Young TSA), during the progression of DMD (DMD Ageing) and by TSA at Old (Old TSA).
Interestingly, we find that the regions acetylated by Young TSA in AcH3K9/14 contain different specific motif for TFs such as FOXO, STAT and MEF. During DMD progression, FAPs acquire peaks that have specific motifs for the members of the AP-1 complex: JUN and FOS. Old TSA instead specifically acetylates loci for factors of the KLF and E2F family and shows an enrichment for MAZ. Moving forward to the AcH3K27, is interesting to note a lot of the same motifs found for AcH3K9/14 were also discovered here. The loss of acetylation of Young TSA and ageing make FAPs lose a great number of binding sites for the found TFs. This effect is more pronounce during DMD progression as four times the peaks are lost compared to Young TSA. After Old TSA treatment instead, more than four thousand AcH3K27 peaks are gained but no significant motif was found to be present other than the MEF factors. Collectively this analysis reveals that TSA treatment hyper-acetylates regions that are bound by different factors depending on the stage of DMD.
Then, in order to obtain highly specific regions that gain or lose acetylation during disease progression and TSA, we performed an overlap analysis, in which we checked the correspondence of the genomic regions belonging to every differential comparison against each other. For example, the Upset graph in Figure 8C shows that out of the 12553 AcH3K9/14 peaks acquired by TSA in Young FAPs, 9383 (see figure 8C, upper graph, red circlet) are specifically acetylated by TSA treatment at this stage, while others

are commonly acetylated also during ageing (≈ 2000) or TSA treatment of Old FAPs (696, see figure 8C, upper graph, blue circlet). This finding suggests that TSA acetylates different regions in a stage-dependent manner. Moving forward, DMD dramatically alters the epigenetic landscape in terms of AcH3K27 as 9520 regions (see figure 8C, lower graph, red circlet) gets depleted of this histone modification. TSA at this stage is able to re-establish only a minor part of those peaks (1518, see figure 8C, lower graph, blue circlet). The analysis showed in Figure 8C also set the fundaments to arrange a panel of a restricted set of specific loci for ChIP-qPCR validation. In particular, we are interested in validating the most significative regions of "HDACi responsiveness" (e.g. Young TSA specific peaks), DMD progression (e.g. Young and Old CTR specific peaks) and "HDACi resistance" (e.g. Old TSA specific peaks). Additionally, once validated the effective specificity of these differentially acetylated sites, we aim to test whether they may be used to predict the stage of disease progression and HDACi responsiveness.

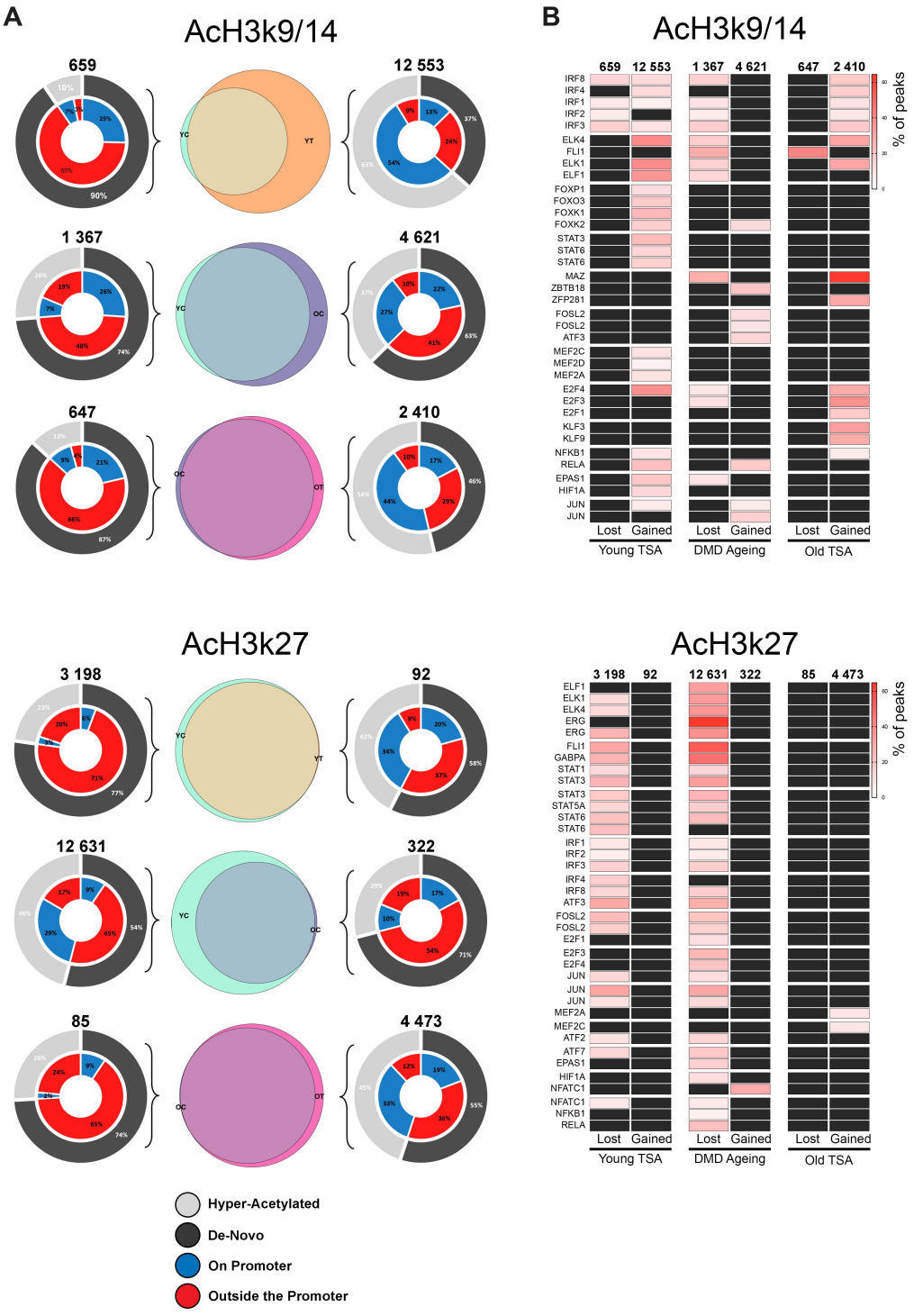
A
AcH3k9/14
659
12 553
1 367
4 621
647
2 410
YC
YT
OC
OT
B
AcH3k9/14
659 12 553
1 367 4 621
647 2 410
% of peaks
Lost Gained
Young TSA
DMD Ageing
Old TSA
AcH3k27
3 198
92
12 631
322
85
4 473
Hyper-Acetylated
De-Novo
On Promoter
Outside the Promoter

c

AcH3k9/14

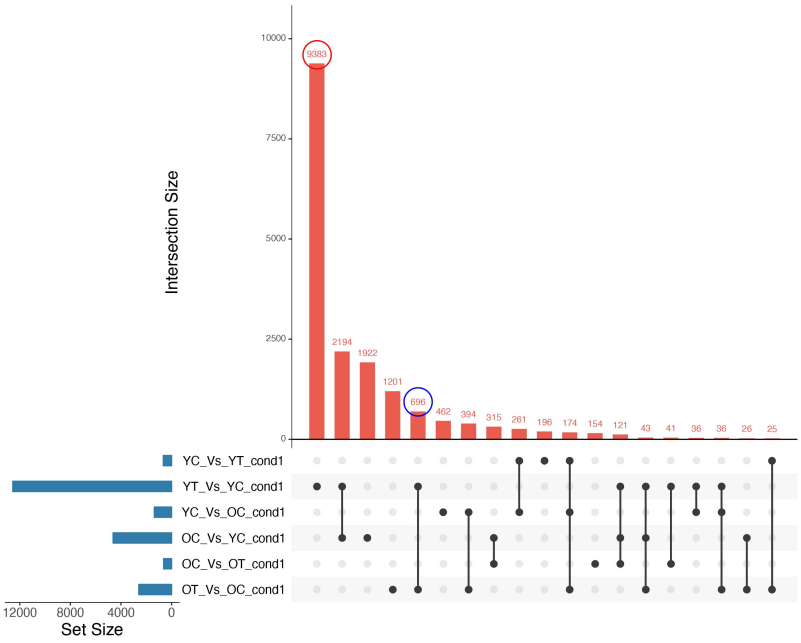

AcH3k27

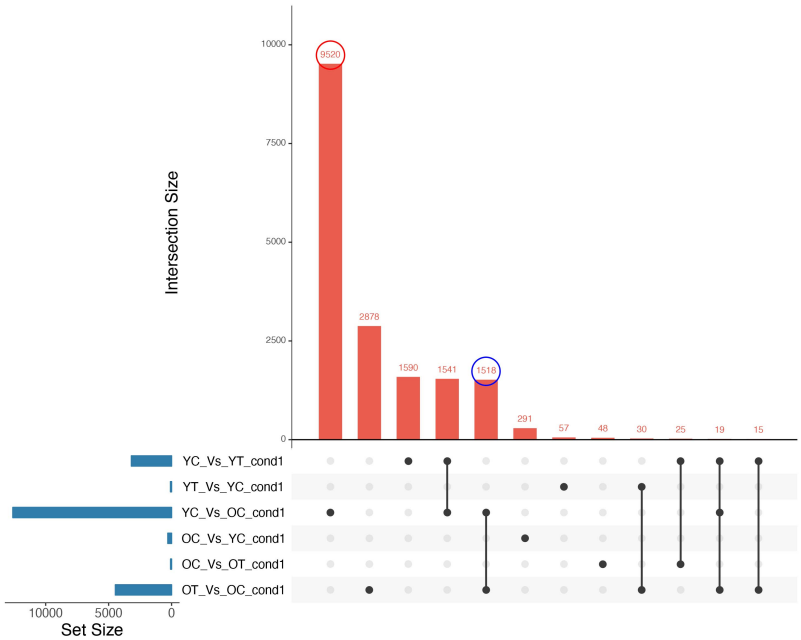

Figure 8: The Epi-Signature of HDACis.
A) Graphic visualization of differential analysis for both AcH3k9/14 - upper panel - and AcH3k27 - bottom panel - of FAPs 1.5 Months old control against FAPs 1.5 Months old TSA - First row -, FAPs 1.5 Months old control against FAPs 12 Months old control - second row - and FAPs 12 Months old control against FAPs 12 Months old TSA - third and last row-. The Venn diagrams represent the proportion of the differential peaks compared to the common peaks. The double donut graphs surrounding each Venn diagram represent the type of acetylation - Hyper-acetylation in grey and De-novo acetylation in Black - for the outer layer and the acetylation distribution - On the promoter in blue and outside the promoter in red - for the inner layer. **B)** Heatmap representing the % of peaks (for either AcH3k9/14 - upper panel - and AcH3k27 - bottom panel -) containing specific motifs for DNA binding factors. The Motifs are clustered by protein family and ordered by the most abundant motif family to the least one. Only protein families with more than 1 members were taken into account. On top of each column are reported the number of peaks characteristic of each dataset. **C)** Upset graph representing the intersection of the differentially acetylated peaks against each other for both AcH3k9/14 - upper panel - and AcH3k27 - bottom panel. The horizontal histograms in blue reports the number of peaks originally from the differential analysis while the vertical histograms in red account for the intersection size, which is the number of peaks featuring every intersection. Only intersections having more than 20 peaks are shown. The red and blue circlets highlight the intersections mentioned in the manuscript.

4.3 TSA modulates different genes in a DMD stage-dependent fashion

We then questioned whether the epigenetic changes imposed by TSA at different stages of DMD progression result in significant transcriptomic changes. Therefore, we performed an RNA-seq experiment in the same ChIP-seq samples. By plotting the most modulated genes in Principal Component Analysis (PCA) we could clearly appreciate that most of the transcriptomic changes in FAPs occur during the progression of the pathology (Figure 9A). The first component of variance (PC1, 88% of variance) clearly discriminates Young FAPs from Old FAPs. The second component of variance (PC2, 6% of variance) instead, reflects the treatment with TSA and shows a more pronounced effect in Young FAPs compared to Old FAPs (Figure 9A). By performing Gene Ontology analysis on the genes that characterize the PC-1 and PC-2 we observed that DMD ageing and TSA treatment modulate different subset of biological functions. For instance, in the PC-1 Gene Ontology we found terms related to response to stimuli, cell stress, cell death and migration, while the PC-2 is mainly characterized by modulation of chromatin conformation, cell cycle and muscle tissue development (Figure 9B and C). Interestingly, the regulation of cell proliferation is a shared biological process between PC-1 and PC-2. We then performed DESeq2 analysis to identify the genes differentially modulated by TSA during the progression of the pathology in dystrophic FAPs (Young TSA and Old TSA, Figure 9D and E). Interestingly, the treatment induces both up and down regulation of gene expression with a slight increase in down-regulated genes by Old TSA. This result seems counterintuitive at first as TSA, being an HDACi, is expected to only up-regulate target genes. Our speculation is that the down-regulation is the consequence of an indirect effect of TSA treatment, due for example to hyper-acetylation and up-regulation of genes that consequently inhibit downstream factors. In this way HDACi

would indirectly affect the expression of secondary target genes in both directions.
We then compared the differentially expressed genes modulated by TSA in young and old mdx FAPs. As highlighted by the red circlets in the venn diagram of Figure 9F, TSA selectively modulates different subset of genes at early and late stages of DMD. Collectively this data suggests that besides a different epigenetic profile, HDACi modulate gene expression in dystrophic FAPs in a completely different manner depending on the progression of the pathology. The validation of genes of interest is required to confirm this data though.

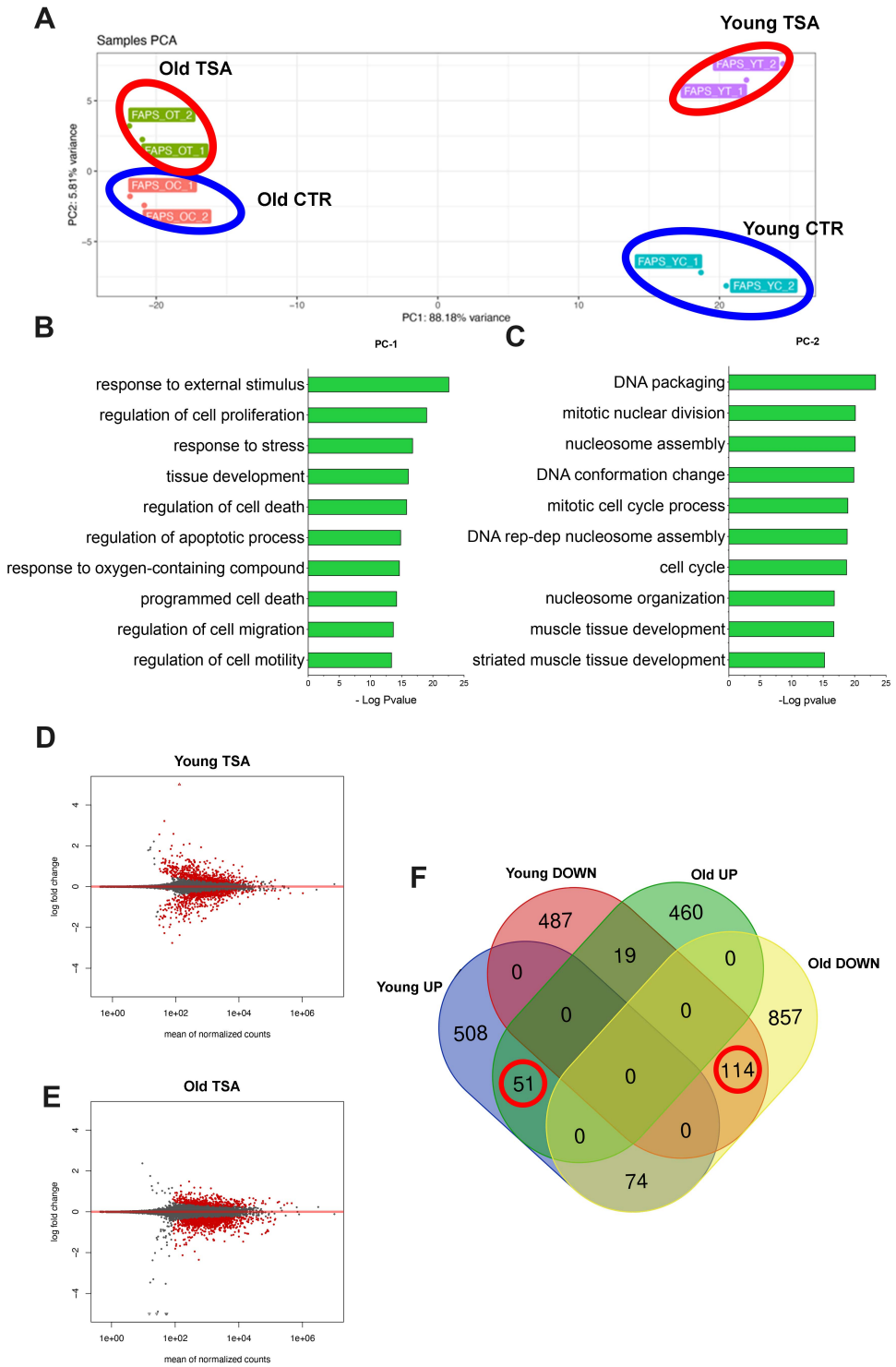
A
Samples PCA
Young TSA
Old TSA
Old CTR
Young CTR
FAPS_YT_2
FAPS_YT_1
FAPS_OT_2
FAPS_OT_1
FAPS_OC_1
FAPS_OC_2
FAPS_YC_1
FAPS_YC_2
PC2: 5.81% variance
PC1: 88.18% variance
B
PC-1
response to external stimulus
regulation of cell proliferation
response to stress
tissue development
regulation of cell death
regulation of apoptotic process
response to oxygen-containing compound
programmed cell death
regulation of cell migration
regulation of cell motility
- Log Pvalue
C
PC-2
DNA packaging
mitotic nuclear division
nucleosome assembly
DNA conformation change
mitotic cell cycle process
DNA rep-dep nucleosome assembly
cell cycle
nucleosome organization
muscle tissue development
striated muscle tissue development
-Log pvalue
D
Young TSA
log fold change
mean of normalized counts
E
Old TSA
log fold change
mean of normalized counts
F
Young DOWN
Old UP
Young UP
Old DOWN
487
460
19
0
0
0
0
857
508
51
0
114
0
0
74

Figure 9: Transcriptomic changes during DMD progression and TSA treatment
A) Principal component analysis performed on the most 1000 regulated genes using the tool "PcaExplorer" on FAPs Young CTR (YC), Old CTR (OC), Young TSA (YT) and Old (TSA). **B)** Gene Ontology performed on the modulated genes for the PC-1 and **C)** PC - 2. **D)** Volcano Plot representing the differentially expressed genes (dots) log fold change of the treatment of TSA in young mdx FAPs (Young TSA) and **E)** old mdx FAPs (Old TSA). Genes with PADJ < 0.1 are shown represented by red dots. **F)** Venn diagram showing the overlap of the differentially expressed genes between the treatment of TSA at early stages (Young UP and DOWN) and late stages (Old UP and DOWN) in FAPs.

4.4 Biological functions prediction reveals the inverse relationship of TSA treatment effect at early and late stages of DMD

Until now we have dissected the different epigenetic and transcriptomic events executed by TSA at early and late stages of DMD. At this point we sought to understand their biological meaning and relationship to the stage-dependent beneficial effects executed by HDACi in DMD pathology [23,101].
We therefore integrated ChIP and RNA-seq analysis to label, in terms of Gene Ontologies, the main biological functions affected by TSA treatment in FAPs. The results of the integration are described in Figure 10A where we observed that TSA hyper-acetylates promoters of both up and down regulated genes. As already suggested for Figure 9 D and E, it is possible that such effect may be due to downstream factors activated by TSA.
Further analysis of validation will be needed to confirm this theory though. Notably, roughly 50% of young TSA up-regulated genes are hyper-acetylated while only 10% of old TSA up-regulated genes show an increase in histone acetylation.
Then, taking advantage of Ingenuity Pathways Analysis technology (IPA), we identified the main categories of biological functions significantly modulated by TSA treatment (Figure 10B). We explored their predicted regulation exploiting both our whole transcriptomic dataset and its integration with AcH3K9/14 and AcH3K27 ChIP-seq. The integrative analysis discovered the subset of genes in which the acetylation profile is consistent with the expression pattern: downregulated genes with hypo-acetylated promoters and upregulated genes with hyper-acetylated promoters.
The results of this analysis are summarized by the double gradient heatmap in figure 10B, where the most modulated clusters of biological functions are shown: Gene expression, Cell Cycle, Cell to cell interaction, Cell Movement, Cell Tissue and Development and Cell Death and survival. The inverse relationship between the transcriptomic modulation imposed by TSA in young and in old

FAPs on any-singular biological function, is quite striking. Briefly, TSA treatment in young mdx FAPs (Young TSA) is predicted to promote gene expression, cell cycle progression, cell interaction, cell migration, myogenesis and cell survival, while negating cell death and adipogenesis. TSA treatment in old mdx FAPs (Old TSA) is predicted to behave exactly in the opposite direction.
Notably, some of these biological functions are already known to be modulated by TSA in young dystrophic FAPs, supporting the power of the analysis. Indeed HDACis have previously been shown to potentiate muscle regeneration by enhancing the FAPs to MuSCs functional crosstalk and reducing FAP adipogenic potential at early but not late stages of DMD [101].
Analogous modulation of such biological functions is also predicted by the subset of genes revealed by RNA/ChIP-seq data integration. Accordingly, to the acetylome profile, Young TSA activity is highly dependent H3K9/14 promoter hyper-acetylation, while Old TSA is partially dependent on both H3K9/14 and H3K27 histone acetylation. This analysis suggests that the epigenetic remodeling, enforced by TSA in mdx FAPs, is indeed responsible of the modulation of the mentioned biological functions.

A

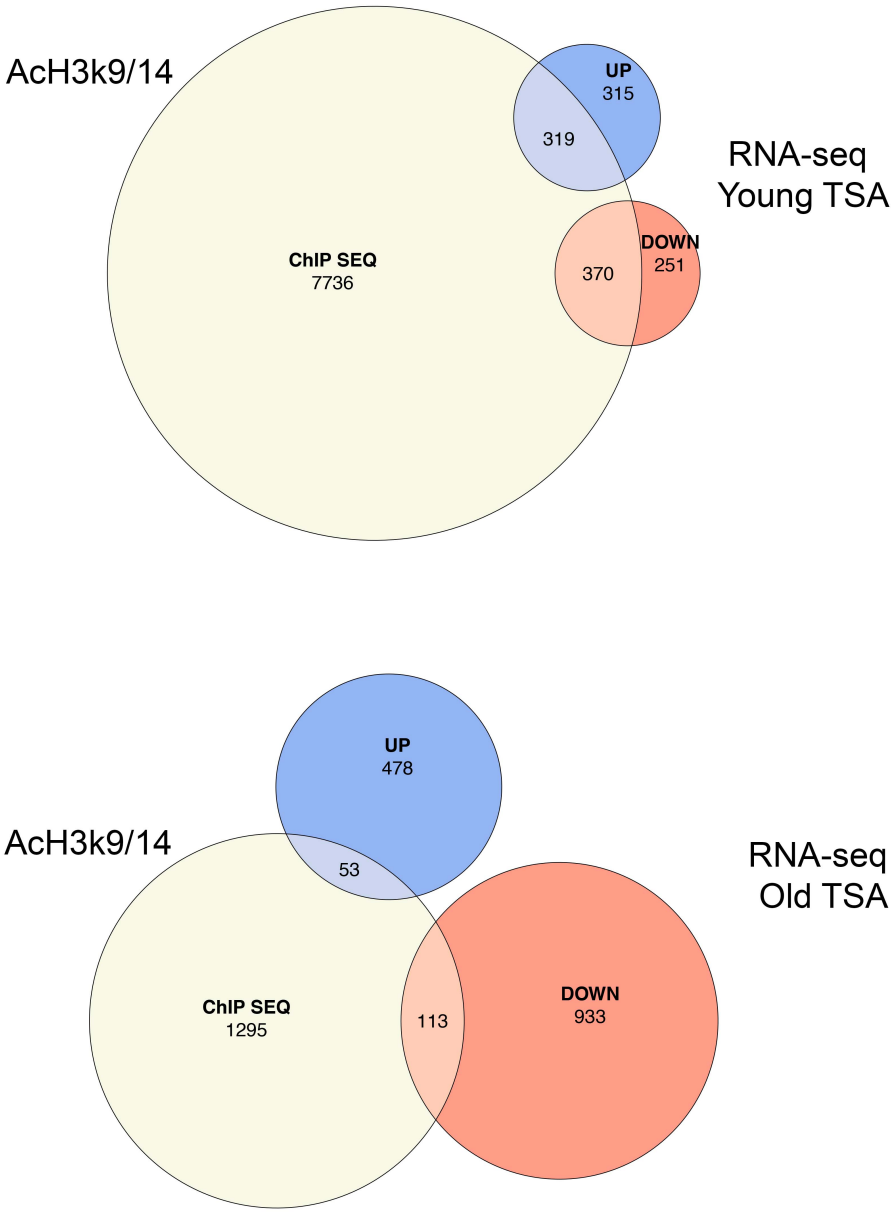
AcH3k9/14
UP
315
319
RNA-seq
Young TSA
ChIP SEQ
7736
DOWN
251
370
UP
478
AcH3k9/14
53
RNA-seq
Old TSA
ChIP SEQ
1295
113
DOWN
933

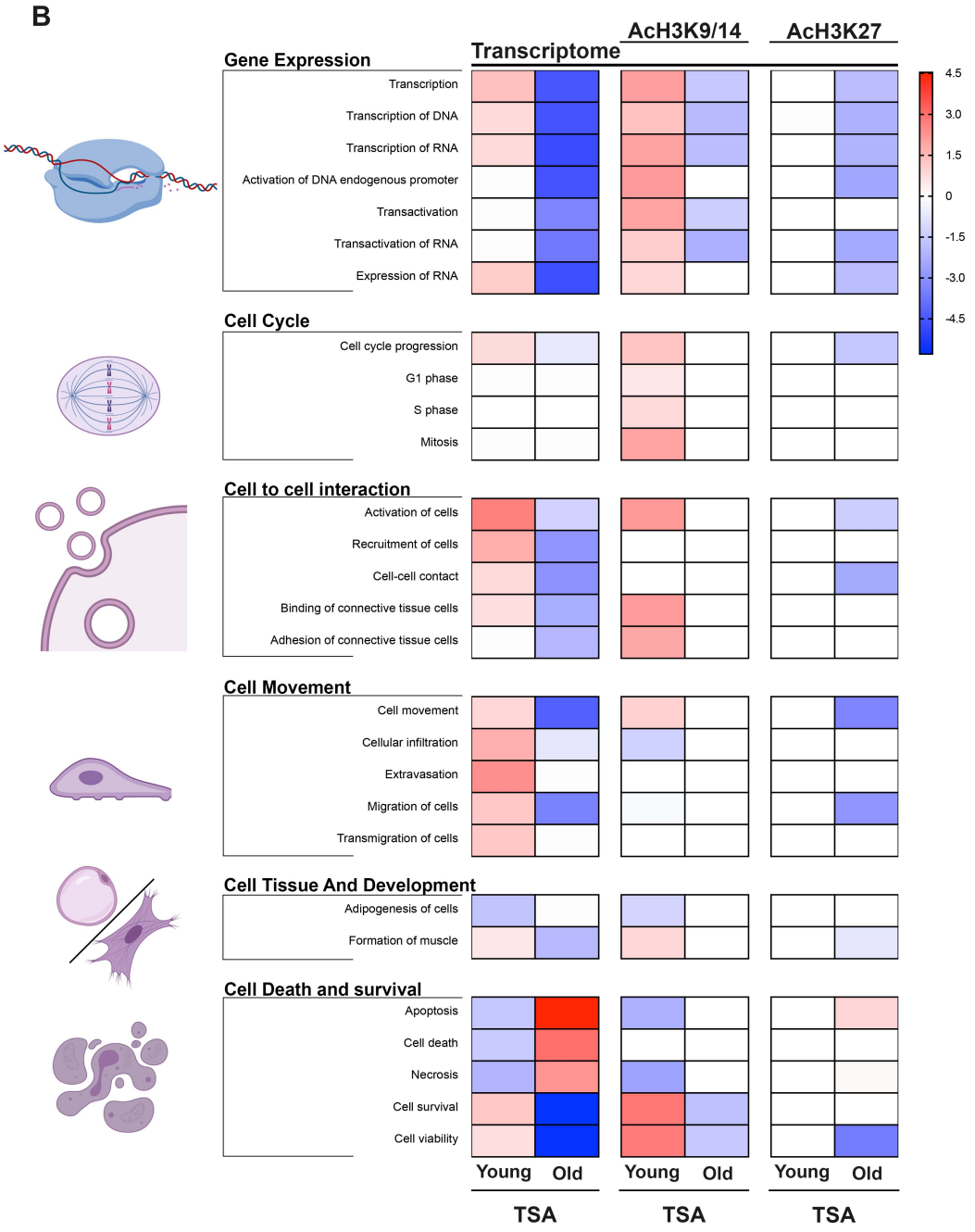
B
Transcriptome
AcH3K9/14
AcH3K27
Gene Expression
Transcription
Transcription of DNA
Transcription of RNA
Activation of DNA endogenous promoter
Transactivation
Transactivation of RNA
Expression of RNA
Cell Cycle
Cell cycle progression
G1 phase
S phase
Mitosis
Cell to cell interaction
Activation of cells
Recruitment of cells
Cell-cell contact
Binding of connective tissue cells
Adhesion of connective tissue cells
Cell Movement
Cell movement
Cellular infiltration
Extravasation
Migration of cells
Transmigration of cells
Cell Tissue And Development
Adipogenesis of cells
Formation of muscle
Cell Death and survival
Apoptosis
Cell death
Necrosis
Cell survival
Cell viability
Young
Old
TSA
4.5
3.0
1.5
0
-1.5
-3.0
-4.5

Figure 10: Biological functions prediction reveals the inverse relationship of TSA treatment effect at early and late stages of DMD.
A) Proportional venn diagrams showing the integration of the H3K9/14 hyper-acetyleted peaks on the promoters (ChIP-seq) with the differentially expressed genes (up regulated - UP- and down regulated - DOWN -) of TSA treatment in young mdx FAPs - upper venn diagram - and in old mdx FAPs - lower venn diagram -. **B)** Heatmap representing the activation (Red) or inhibition (Blue) of the most significative clusters of biological functions modulated in mdx FAPs after TSA treatment at either early stages (Young TSA) or late stages (Old TSA) of DMD. The heatmap was generated in Ingenuity Pathway Analysis (IPA) uploading the differentially expressed genes by RNA-seq (first two rows) and by integrating those genes with the ChIP-seq peaks for AcH3k9/14 (two middle rows) and AcH3k27 (last two rows).

4.5 Predictive analysis suggests that TSA at early stages of DMD may terminate putative Fibro-Enhancers

We further extended the analysis of the main biological functions modulated by TSA with an exploratory study of putative enhancers. Analysis of H3K27 acetylation profile previously revealed that TSA treatment leads to the loss of 3198 peaks in young mdx FAPs, while the acquisition of 4473 peaks in old mdx FAPs. Taking advantage of Genomic Regions Enrichment of Annotations Tool (GREAT) we were able to assign putative enhancers (defined as peaks for AcH3K27 outside the promoter boundaries) to predicted promoter regions. Interestingly, the distribution of enhancer-promoter looping suggests that the putative enhancers dismissed by TSA in young mdx FAPs interacts with more promoters compared to the putative enhancers gained by TSA in old mdx FAPs (Figure 11A). Assuming that gained enhancer-promoter interaction should lead to gene up-regulation and vice versa, we integrated the list of GREAT-predicted modulated genes with the list of differentially expressed genes by RNA-seq (Figure 11B). Out of the 527 predicted repressed genes, 251 are effectively downregulated in young TSA FAPs (an overlap of approximately 50%), while only 16% of the predicted activated genes are found upregulated in old TSA FAPs (Figure 11B).

By performing Gene Ontology on the predicted repressed genes by young TSA we found terms involved in fibrosis, such as cell matrix adhesion and extracellular matrix organization (Figure 11C). In addition, two out of the top three most interacting promoters are collagen genes (Col5a2 and Col3a1, Figure 11A).

Our speculation is that one of the layers of TSA effectiveness at early stages of DMD is the termination of putative fibro-enhancers, unveiling a dual mechanism by which HDACi control adipogenesis and fibrogenesis in FAPs by respectively modulating promoter and enhancer commitment.

On the other hand, AcH3K27 gained by TSA at advanced stages of DMD results in less productive interactions and less accordance with up-regulated genes. Interestingly motif discovery in these loci

previously failed in identifying significant transcription factors involved in their regulation (Figure 8B) supporting their meaningless function. It is important to note that in order to confirm our speculations the putative enhancers and the enhancer promoter looping described in this explorative analysis need experimental validation. In order to validate the enhancers identity, we plan to perform ChIP-qPCR for AcH3k4me1 and AcH3k27; while to test enhancer-promoter interaction 3C/4C or FISH experiments are necessary.

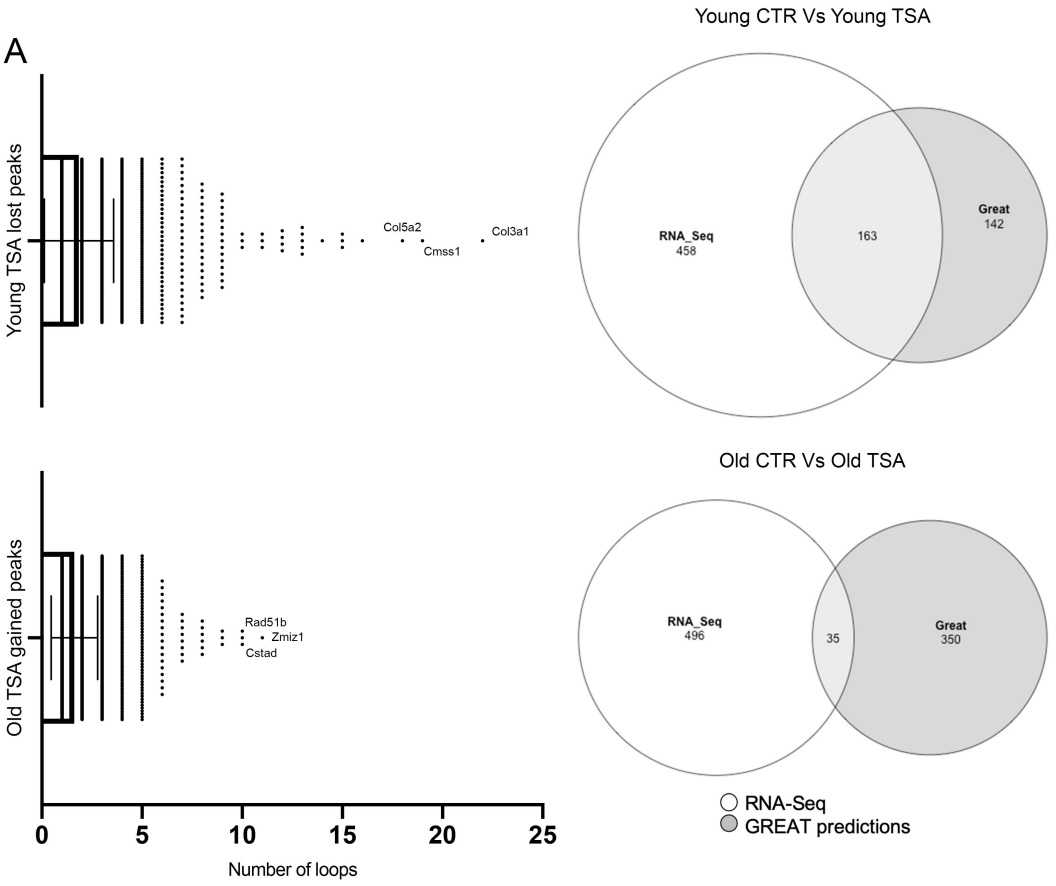
A
Young TSA lost peaks
Col5a2
Cmss1
Col3a1
Old TSA gained peaks
Rad51b
Zmiz1
Cstad
0
5
10
15
20
25
Number of loops
Young CTR Vs Young TSA
RNA_Seq
458
163
Great
142
Old CTR Vs Old TSA
RNA_Seq
496
35
Great
350
RNA-Seq
GREAT predictions

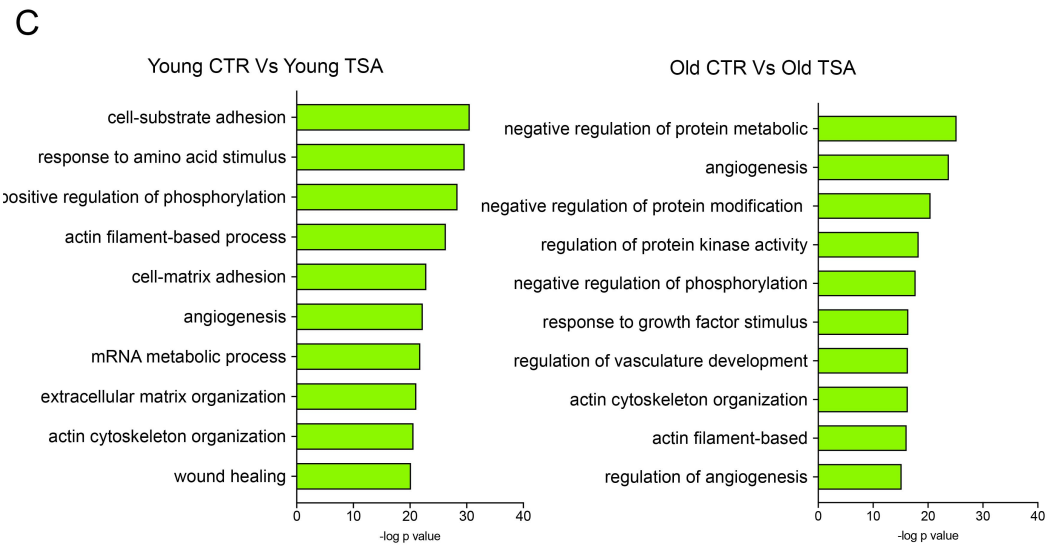
C
Young CTR Vs Young TSA
cell-substrate adhesion
response to amino acid stimulus
positive regulation of phosphorylation
actin filament-based process
cell-matrix adhesion
angiogenesis
mRNA metabolic process
extracellular matrix organization
actin cytoskeleton organization
wound healing
0
10
20
30
40
-log p value
Old CTR Vs Old TSA
negative regulation of protein metabolic
angiogenesis
negative regulation of protein modification
regulation of protein kinase activity
negative regulation of phosphorylation
response to growth factor stimulus
regulation of vasculature development
actin cytoskeleton organization
actin filament-based
regulation of angiogenesis
0
10
20
30
40
-log p value

Figure 11: TSA at early stages of DMD terminate putative Fibro-Enhancers
A) Box plots representing the distribution of the Promoters - Putative Enhancers interactions (Number of loops) for peaks lost by TSA at 1.5 Months of age (Young TSA lost peaks) and the peaks gained by TSA at 12 Months of age (Old TSA gained peaks) for AcH3K27 in MDX FAPs. The gene names of the top 3 promoters are also shown. **B)** Proportional Venn diagrams representing the integration between the RNA-seq (White circle) and the GREAT-predicted regulated genes that were significantly modulated (Padj < 0.1) by RNA-seq in FAPs. The overlap between the datasets reports the number of genes that are modulated accordingly with the GREAT prediction: - Young CTR Vs Young TSA - Genes predicted to be downregulated by the absence of predicted putative enhancers after TSA treatment at 1.5 months of age; - Old CTR Vs Old TSA - Genes predicted to be upregulated by the acquisition of predicted putative enhancers after TSA treatment at 12 months of age. **C)** Gene Ontology by GREAT analysis of the genes predicted to be modulated by putative enhancers.

4.6 TSA promotes the activation of a long-lasting cell cycle

In Figure 7 and 8 we unveiled the epigenetic signature of HDACis efficacy: a massive hyper-acetylation in H3K9/14 on more than 9000 specific loci preferentially located on gene promoters. The same epi-signature is also responsible for the modulation of the main biological functions in young mdx FAPs by TSA (figure 10B). We further aimed to reveal the identity of the genes specifically modulated by early-stage TSA treatment. We therefore integrated its unique 9383 hyper-acetylated peaks with the most significantly up-regulated genes by RNA-seq and found as the most representative gene family the "Replication-dependent histone variants" belonging to the first cluster of histones (HIST1). This cluster of histone proteins is basically down-regulated during disease progression or not affected by TSA treatment at late stages of DMD (Figure 12 A).

Consistently, we found the canonical pathway "Cyclins and Cell Cycle Regulation" as significantly activated in young FAPs treated with TSA by IPA analysis of the transcriptome. This pathway was repressed in old FAPs or not modulated in old FAPs treated with TSA (Figure 12B).

These results, together with the predicted activation of cell cycle progression (shown in figure 10B), suggest that TSA at early stages pushes FAPs towards cell cycle activation and that replication-dependent histone proteins may serve as new scaffolds for the novel chromatin arrangement imposed by TSA.

Then, to further investigate the role of cell proliferation in TSA treatment, we performed an *in vivo* EdU experiment in young and old mdx mice. Mice were treated with TSA or its vehicle of control for 15 days and injected with EdU solution 24 hours before the sacrifice. EdU is a thymidine analogue which is incorporated into the DNA of dividing cells, representing a valid marker to monitor the rate of cell proliferation.

Immunofluorescence on muscle sections revealed the presence of EdU positive muscle-resident cells. Surprisingly their detection

was strongly reduced in young mdx mice treated with TSA, while old mdx mice showed a partial decline in proliferating cells regardless of TSA treatment (Figure 12C). We attempted to assign EdU signal in FAPs by co-immunofluorescence for Sca-1 (FAP' specific lineage marker). However, we found EdU mainly associated to sub-laminar MuSCs or Sca-1 negative cells (Figure 12D). We therefore took advantage of flow cytometry to univocally profile at single-cell level EdU up-take in FAPs vis-a-vis to MuSCs (Figure 12E). Whole muscles were digested to release mono-nucleated cells and stained for EdU and cell-specific antigens. The analysis confirmed that MuSCs exhibit a higher proliferation rate, since ≈17% experienced cell division in 24 hours compared to ≈5% of FAPs. Both MuSCs and FAPs of young mdx mice slowed down their proliferation rate upon TSA treatment, and accordingly to the previous observation in muscle sections, this effect correlates with the stage-specific activity of HDACi, being proliferation of old cells not significantly affected by TSA.
Reduction in cell proliferation rate is expected to lead to cell depletion, therefore we analyzed the availability of mononuclear cells isolated by young and old dystrophic muscles exposed to TSA (Fig 12F, G). We discriminated Lin+ cells (CD45, CD31 and Ter119 positive cells) including hematopoietic cells, endothelial cells and erythrocytes; Lin-, Sca1-, α7-Integrin+ MuSCs and Lin-, Sca1+, α7-Integrin- FAPs. Respective cell percentages did not change across the samples, showing that no population prevailed the others during disease progression and TSA treatment (Fig 12F). Interestingly, besides the strong decrease in EdU+ cells, TSA did not affect the total number of cells, while a significant reduction in all cell availability is observed at late stages of DMD. This data demonstrates that disease progression affects the proliferative potential of muscle-resident cells leading to a drastic numeric reduction. By contrast, our speculation is that TSA exerts a stage-dependent activity promoting a long-lasting cell cycle without affecting cell availability. This result is conceivable only taking into account the ability of TSA to recruit and activate a massive

number of cells, as suggested by our previous biological function analysis (Figure 10B).
We also observed that TSA reduces the proliferation rate in both MuSCs and FAPs, suggesting a direct effect of the treatment on both cell populations. Since FAP activity strongly influences MuSC expansion and myogenic differentiation, we speculate that this outcome also relies on the increased ability of FAPs exposed to TSA to activate and commit MuSCs toward differentiation [23,101].
Noteworthy, we found that MuSCs exhibits a higher proliferative potential compared to FAPs, but their total number is significantly lower (≈ 1:5). This data reflects their distinct functions in the context of muscular regeneration: MuSCs are massively required for both creating/repairing myofibers while replenishing the stem cell reservoir, whereas FAPs are mainly involved in MuSCs coordination, prospecting a scenario in which fewer "main characters" are supported by a large number of supportive "side characters".

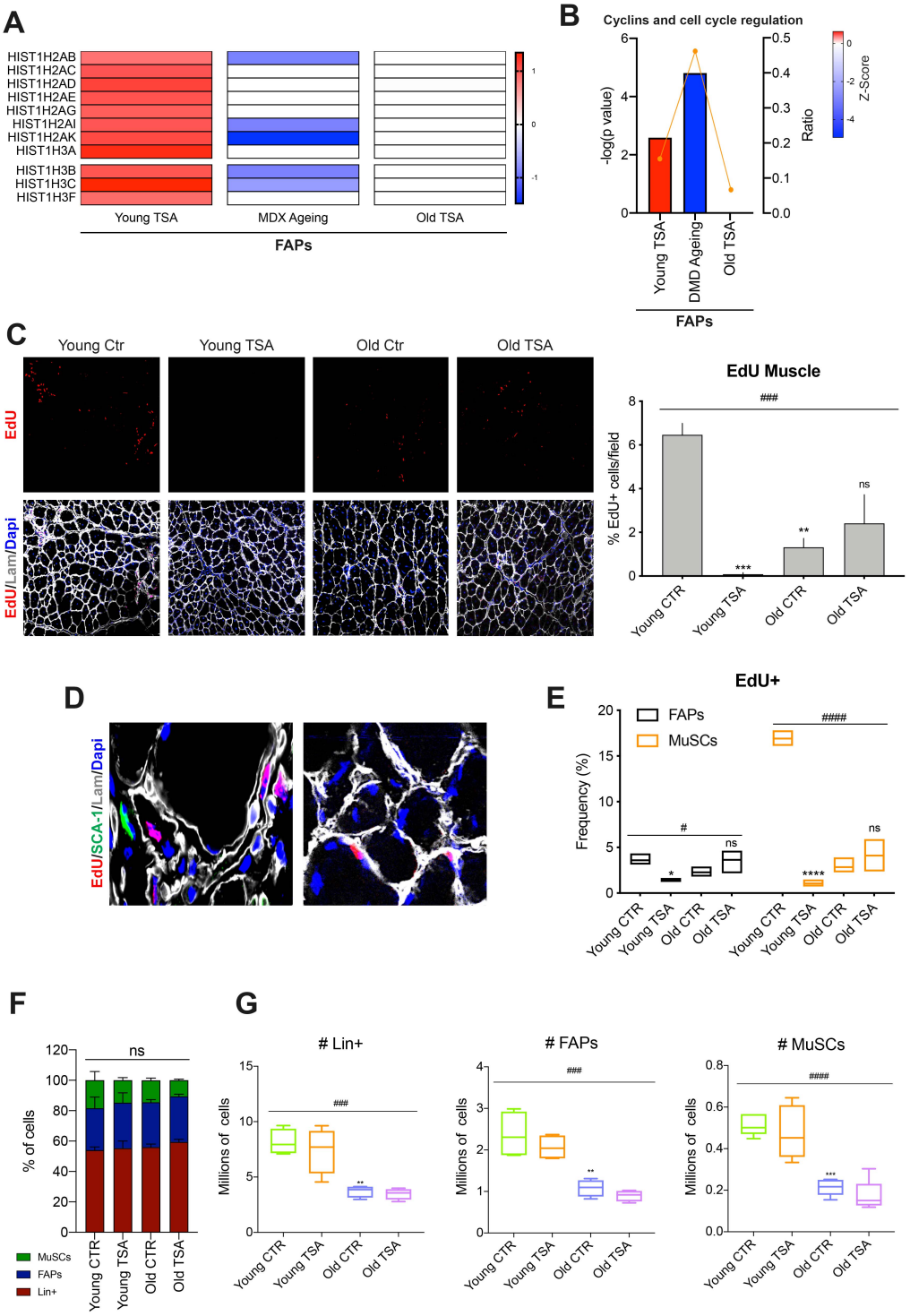
A
HIST1H2AB
HIST1H2AC
HIST1H2AD
HIST1H2AE
HIST1H2AG
HIST1H2AI
HIST1H2AK
HIST1H3A
HIST1H3B
HIST1H3C
HIST1H3F
Young TSA
MDX Ageing
Old TSA
FAPs
B
Cyclins and cell cycle regulation
-log(p value)
Ratio
Z-Score
Young TSA
DMD Ageing
Old TSA
FAPs
C
Young Ctr
Young TSA
Old Ctr
Old TSA
EdU
EdU/Lam/Dapi
EdU Muscle
% EdU+ cells/field
Young CTR
Young TSA
Old CTR
Old TSA
D
EdU/SCA-1/Lam/Dapi
E
EdU+
FAPs
MuSCs
Frequency (%)
F
% of cells
MuSCs
FAPs
Lin+
G
Lin+
FAPs
MuSCs
Millions of cells

Figure 12: TSA promotes a long-lasting cell cycle
A) Heatmap representing the upregulation (Red) or downregulation (Blue) of the most significantly modulated family of genes integrated with the uniquely hyper-acetylated peaks for AcH3K9/14 in FAPs young TSA (FAPs Young TSA), alongside their expression in old FAPs CTR (MDX ageing) and old FAPs old TSA (FAPs Old TSA). **B)** Composite graph of the IPA Canonical pathway of "cyclins and cell cycle regulation" for FAPs young TSA (FAPs Young TSA), FAPs old CTR (DMD ageing) and FAPs old TSA (FAPs Old TSA). The height of the histograms shows the statistical significance of the pathway modulation (expressed in -log (p value)); the color of the histograms shows the activation (Red) or inhibition (Blue) of the pathway; while the orange dot plot shows the relative amount of genes differentially modulated by RNA-seq and belonging in the pathway. **C)** Left panel: Representative images of EdU staining (Red) in correlation with Laminin (Grey) of muscular cryosections of 1.5 months old mdx mice treated with control (Young CTR) or TSA (Young TSA) and 12 months old mdx mice treated with control (Old CTR) or TSA (Old TSA). The nuclei were counterstained with dapi. The *in vivo* EdU pulse was performed 24 hours before the sacrifice. Right panel: Quantification in % of EdU+ cells per field of the immunostaining in the left panel. **D)** Example image of the Immunostaining for EdU (Red), SCA-1 (Green) and Laminin (Gray) performed to assess the EdU+ FAPs and MuSCs. **E)** Box plot representing the % of EdU + FAPs (Black boxes) and MuSCs (Orange boxes) analyzed with a cytofluorimetric approach on the same experimental points discussed in C. **F)** Quantification of the % of Lin+ cells, FAPs and MuSC. **G)** Quantification of the absolute number of Lin+ cells (Left graph), FAPs (Middle graph) and MuSC (Right graph). Data are represented as average ± SEM, (n=3). * $p< 0.05$, ** $p<0.01$, *** $p<0.001$, **** $p<0.0001$ against Young CTR via T-test, and # $p< 0.05$, ### $p<0.001$, #### $p<0.001$ via one or Two Way Anova.

We further explored the impact of TSA treatment on cell proliferation *ex-vivo*. FAPs isolated from young and old mdx mice treated or not with TSA for 15 days were cultured and after three days exposed to EdU for 6 or 24 hours (Figure 13A).
First, we noticed that old FAPs extrapolated from their muscular environment show an impaired ability to attach and survive. Indeed, even if the cells were plated simultaneously and in equal number for all the experimental conditions, a lower number of old FAPs compared to young was found adherent and round shaped after 24 hours (Figure 13B, C). In the following days, only a small

fraction of old FAPs survived and entered the cell cycle. Interestingly, as anticipated by the predicted biological functions (Figure 10B), TSA exacerbated their mortality (Figure 13 D-F).
By contrast young FAPs succeed to efficiently attach, acquired a flat morphology (Fig.13B, C) and started proliferating (Figure 13 D-F).
According to our previous *in vivo* data, we observed that TSA treatment slowed the proliferation rate of young FAPs, as a lower number of cells incorporated EdU after 6 hours (Figure 13 D-E) and the duplication time of FAPs isolated from *in vivo* TSA treated young mdx mice is doubled compared to the control (Figure 13 G). On the other hand the EdU incorporation alteration was almost totally recovered in the 24 hours time point, demonstrating that all FAPs still retain the ability to proliferate (Figure 13D, E). As expected, the reduced proliferation rate of FAPs TSA led to a decreased cell number in culture plates (Figure 13D, F). This discrepancy from our *in vivo* experiment suggests the concomitant ability of TSA to activate and recruit an increased pool of FAPs, two biological events that cannot be appreciated in cell cultures, where the same number of cells is plated and inevitably activated.
Noteworthy, "Activation of cells" and "Cell Cycle progression" are two biological functions highly interdependent and promoted by TSA in young FAPs, as predicted by IPA analysis (Figure 10B and Figure 13G). The network of interactions shows the high degree of interconnection between these functions, linked by several genes found modulated in the RNA-seq analysis (Figure 13H). In particular, validation of Mki67 expression profile by qPCR (Figure 13I) and cytofluorimetric analysis of in-vivo expression of Ki-67 (Figure 13J) confirmed the increased commitment of young FAPs toward activation and cell cycle entry upon TSA exposure. Furthermore, the decrease in expression of Ki-67 showed in Figure 13I, supports the progressive impairment and unresponsiveness of old FAPs to TSA.

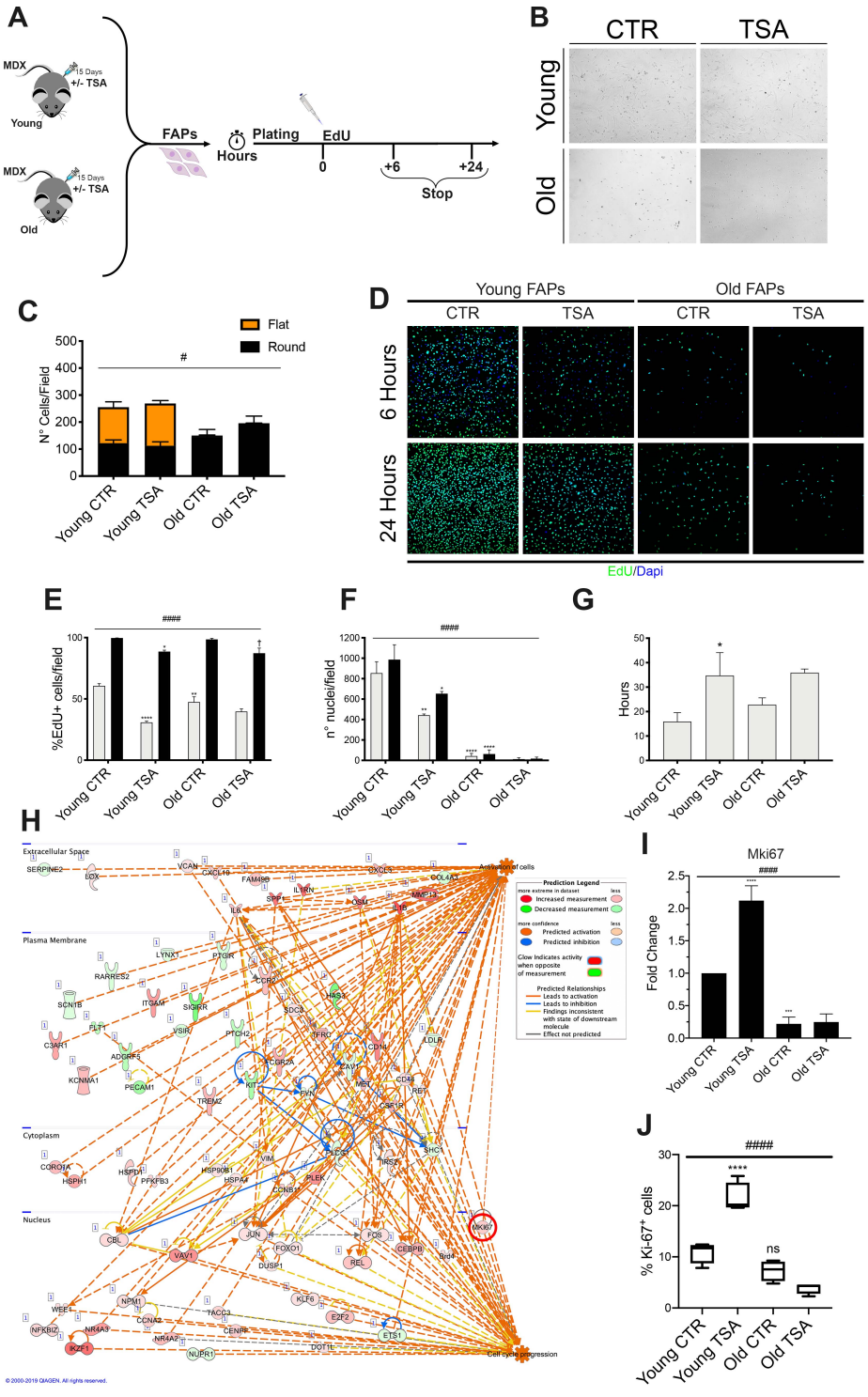
A
MDX
15 Days
+/- TSA
Young
MDX
15 Days
+/- TSA
Old
FAPs
Hours
Plating
EdU
0
+6
+24
Stop
B
CTR
TSA
Young
Old
C
Flat
Round
N° Cells/Field
#
Young CTR
Young TSA
Old CTR
Old TSA
D
Young FAPs
Old FAPs
CTR
TSA
CTR
TSA
6 Hours
24 Hours
EdU/Dapi
E
%EdU+ cells/field
####
F
n° nuclei/field
####
G
Hours
H
Extracellular Space
Plasma Membrane
Cytoplasm
Nucleus
Prediction Legend
Increased measurement
Decreased measurement
Predicted activation
Predicted inhibition
Predicted Relationships
Leads to activation
Leads to inhibition
Effect not predicted
Cell cycle progression
I
Mki67
####
Fold Change
J
####
% Ki-67+ cells
ns

Figure 13: TSA promotes the activation of FAPs
A) Cartoon representing the experimental plan. Briefly, FAPs from 1.5/12 months old MDX mice (Young and Old FAPs) treated with TSA (TSA) or its vehicle of control (CTR) for 15 days were plated for 72 Hours, then an EdU pulse of 6 hours or 24 hours was performed. **B**) Phase contrast image of the experimental points described in A after 24 hours in culture. **C**) Quantification of the number of cells per field of B. Cells were quantified per morphology (Round and Flat). **D)** Representative images of the EdU staining on FAPs from the experimental points described in A. **E**) Quantification of the % of Edu+ FAPs. Grey histograms represent the time point at 6 hours and the black histograms represent the time point at 24 hours, as described in the legend. **F)** Quantification of the number of Nuclei/Field, Same legend of E applies. **G)** Average of the Duplication time of the cells in D. **H**) Network of interactions generated in IPA linking the biological processes of "Activation of cells" and "Cell Cycle progression". The red circlet highlights Ki-67 (MKI67). The colorimetric legend is on the right. **I**) Fold change of expression compared to the FAPs isolated from 1.5 months old mdx mice of control (FAPs Young CTR) of Ki-67 (MkI67). **J)** Cytofluorimetric analysis of *in vivo* Ki-67 expression in young and old mdx FAPs treated with TSA (Young/Old TSA) or its vehicle of control (Young/Old CTR) for 15 days. Data are represented as average ± SEM, (n=3). * $p< 0.05$, ** $p<0.01$, **** $p<0.0001$ against Young CTR via Tuckey multiple comparisons test, and # $p< 0.05$, #### $p<0.001$ via one or Two Way Anova.

4.7 HDACis enhances FAPs engraftment and migration when transplanted in early stages dystrophic muscles

DMD is a concert of asynchronous foci of muscle degeneration and regeneration [99]. In the regenerative context at the onset of DMD, we found that FAPs are activated by TSA, but in order to assist MuSC-mediated muscle regeneration, they need to reach the site of damage. Our predictive analysis of biological functions (Figure 10B) suggested that TSA also promotes FAP movement and migration, a novel pharmacological effect never revealed before. Therefore, we decided to gain insight of this function by evaluating FAP migration both *ex-vivo* and *in vivo* (Figure 14A).
We first tested the ability of FAPs to migrate in culture plates by wound healing assay (Figure 14 A-D). As shown in the previous *ex-vivo* EdU experiment (Figure 13 B-F), old FAPs showed impaired cell survival, especially after TSA exposure. For this reason, old FAPs are difficult to compare with young FAPs. Therefore, we performed our preliminary analysis to monitor the migration of FAPs from young mdx mice treated with TSA or its vehicle of control *in vivo*. Isolated FAPs were plated at confluence and then the cell layer was scratched.
We also explored and compared the efficacy of TSA *in vitro*, by treating control FAPs in culture 9 hours before starting the assay. In order to monitor the wound healing, we took pictures at 0, 14, 19, 24 and 48 hours post-scratch (Figure 14B) and measured the percentage of wound filled at the different time points (Figure 14C), and the actual speed of FAP migration (Figure 14D).
FAPs isolated from young mdx mice *in vivo* treated with TSA were able to fill the wound in a quicker and steadier way compared to control FAPs. Interestingly, TSA *in vitro* treatment pushed FAP migration at early time points, but this ability was progressively lost during the assay (Figure 14 B-D). This observation suggests that environmental stimuli might contribute *in vivo* to the stable acquisition of the enhanced migratory phenotype of FAPs.

We therefore set-up an *in vivo* technical approach to further explore FAP migration (Figure 14 A). FAPs were purified from young and old mdx mice *in vivo* treated with TSA or its vehicle of control. Freshly isolated FAPs were stained with the membrane dye PkH-67 and injected into dystrophic muscles at the proximal part to the tendon. Precisely, young and old FAPs (either treated or not with TSA) were respectively injected into young and old mdx host mice. In addition, old FAPs were also injected into young mdx host mice to assess whether the regenerative muscle environment responsive to TSA could influence the behavior of old FAPs. After 5 days, host mdx mice were sacrificed and the injected muscles were cut in three consecutive sections defined as Proximal, Medial and Distal to the site of injection. Taking advantage of the fluorescent labeling of injected FAPs, we were able to monitor their engraftment (Figure 14 E) and migration along the muscle sections by flow cytometry (Figure 14 F). Of note, given the low proliferation rate of FAPs *in vivo* (Figure 13 D-G), experimental outcomes are mainly ascribed to changes in FAP survival and migration more than expansion.
Interestingly, we observed that old FAPs showed a higher engraftment compared to young when transplanted in their respective environment. By contrast, transplantation of old FAPs in young muscles reduced their availability, suggesting the crucial role of external stimuli in modulating their survival (Fig 14 E). Accordingly, previous studies demonstrated the impact of TNF and TGF-beta signals in coordinating FAP death and survival in dystrophic muscles [21]. In these different scenarios, pre-exposure to TSA inversely affected FAP engraftment: in young cells enhanced their availability, while in old reduced their survival (Figure 14 E). This result is highly consistent with the stage-dependent activity of TSA on FAP death and survival anticipated by our predictive analysis of biological functions (Figure 10B). Surprisingly, old FAPs pre-exposed to TSA recovered their engraftment potential when transplanted in young muscles (Figure 14 E), highlighting

the key contribution of muscle environment in deciphering the message delivered by HDACis.
We then explored the ability of FAPs to migrate from the injection site toward the distal muscle section (Figure 14 F). We observed that the vast majority of FAPs resided in the Proximal section independently from the age of the donor and host mdx mice. Pre-exposure to TSA strongly promoted FAP migration toward the Medial and Distal muscle section in young but not old FAPs.
By changing the environment of un-responsive old FAPs we were able to observe a partial recovery of TSA effect on FAP migratory ability, indeed ≈50% of old FAPs TSA moved and reached the Medial section when transplanted in young dystrophic muscles.
Collectively these results demonstrate that TSA modulates FAP survival and migration in a stage dependent manner. Moreover, our data unveils the strong contribution of the muscle environment in determining the phenotypic output of epigenetic treatments.

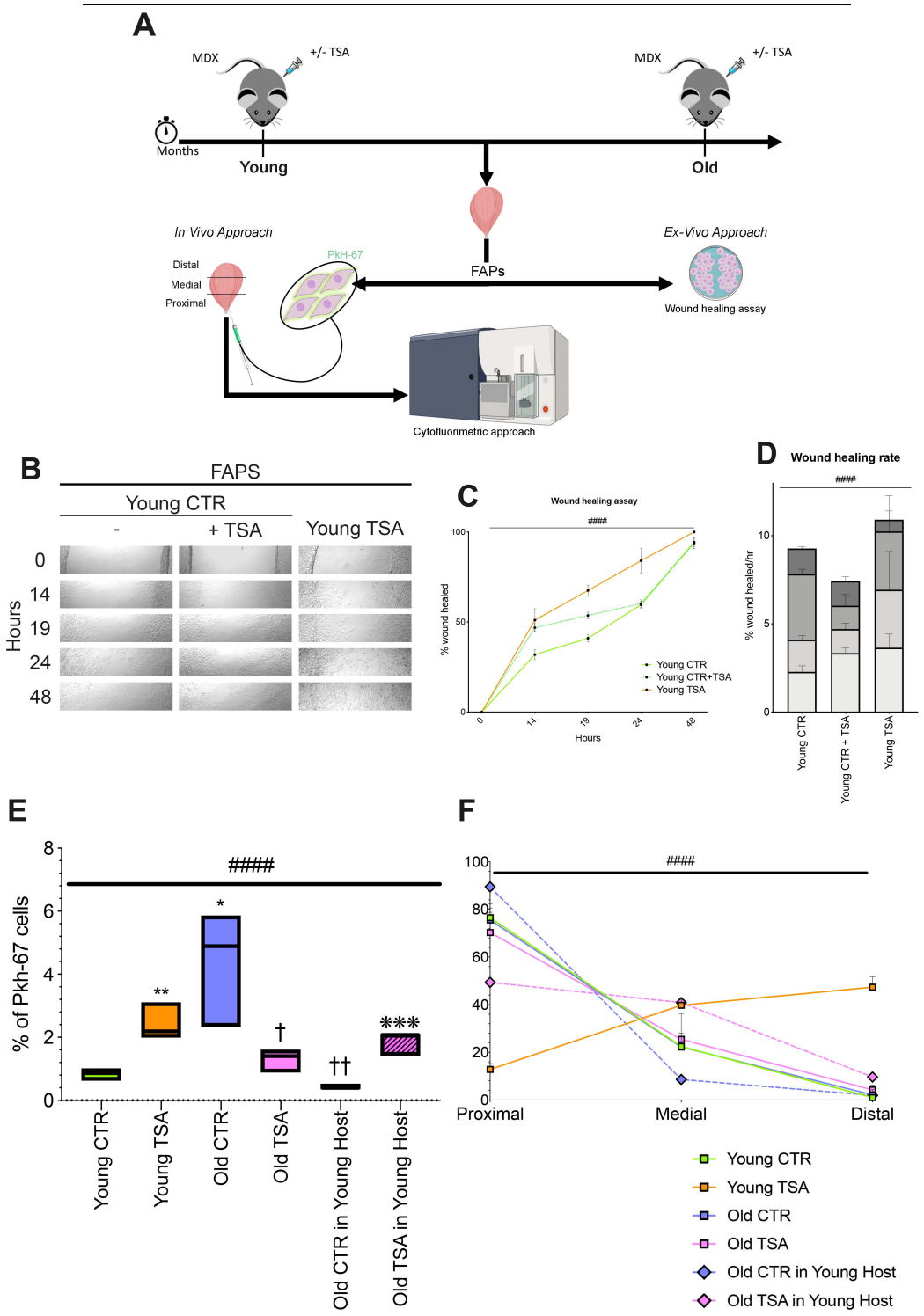
A
MDX
+/- TSA
MDX
+/- TSA
Months
Young
Old
In Vivo Approach
Ex-Vivo Approach
FAPs
Distal
Medial
Proximal
PkH-67
Wound healing assay
Cytofluorimetric approach
B
FAPS
Young CTR
-
+ TSA
Young TSA
Hours
0
14
19
24
48
C
Wound healing assay
####
% wound healed
Young CTR
Young CTR+TSA
Young TSA
Hours
D
Wound healing rate
####
% wound healed/hr
Young CTR
Young CTR + TSA
Young TSA
E
####
% of Pkh-67 cells
Young CTR
Young TSA
Old CTR
Old TSA
Old CTR in Young Host
Old TSA in Young Host
F
####
Proximal
Medial
Distal
Young CTR
Young TSA
Old CTR
Old TSA
Old CTR in Young Host
Old TSA in Young Host

Figure 14: HDACis modulate FAP survival and migration according to different muscle environments.
A) Cartoon representing the experimental plan to asses FAP survival and migration. Briefly, FAPs were isolated from 1.5/12 months old MDX mice treated with TSA or its vehicle of control for 15 days and plated for the wound healing assay (*Ex vivo* approach), or stained with the membrane die "PkH-67" and injected in the gastrocnemius of 1.5 or 12 Months old mdx mice. After 5 days, the muscles were divided in 3 parts from the site of injection (Proximal, Medial, Distal sections) and analyzed by flow cytometry (In vivo approach). **B)** Representative images of the wound healing assay at the different time points (0, 14, 19, 24 and 48 hours post-wound) performed in FAPs from young mdx mice untreated (Young CTR) or treated with TSA (Young TSA) 9 hours prior the wound, control FAPs were treated in-vitro with TSA (+TSA) or its vehicle of control (-). **C)** Graph representing the % of wound healed at the different timepoints. **D)** Graph representing the speed of the migration, expressed in % of wound healed/Hours (hr). **E)** Quantification of the percentage of PkH67+ labeled FAPs in the whole muscles. **F)** Quantification of the percentage of PkH67+ FAPs in the Proximal, Medial and Distal section from the injection site. Data are represented as average ± SEM, (n=3). * $p< 0.05$, * $p<0.01$, against Young CTR and † $p< 0.05$, †† $p<0.01$, against Old CTR; ❋❋❋ $p<0.001$ against Old CTR in Young Host via Tuckey multiple comparisons test; #### $p<0.001$ via one or Two Way Anova.

Discussion

A key feature in the progression of DMD is the initial compensatory response of degenerating muscles through a reactive regeneration that tends to counterbalance muscle loss [119]. HDACis represent the first generation of epigenetic drugs for the treatment of DMD able to counteract disease progression by enhancing muscle regeneration and dwindling fibrosis and adipogenesis [118]. Recent studies from Puri's lab identified FAPs as the main cellular target mediating HDACis efficacy [101] .

FAPs are extremely plastic cells that play a role both in supporting MuSC-mediated muscle regeneration and contributing to the fibrotic and adipogenic degeneration at later stages of DMD.

HDACis promote muscle regeneration by inducing changes in the chromatin of FAPs that suppress their fibro-adipogenic potential and promote their pro-myogenic activity and phenotype [23,101]. However, HDACi beneficial effects are limited to early phases of disease progression, since at advanced stages of disease dystrophic muscles and FAPs showed resistance to the treatment [101]. Until now, the epigenetic and biological mechanisms behind the responsiveness and resistance to the treatment are not completely understood.

Givinostat is an HDACi that has recently entered in phase II/III clinical trials for BMD/DMD on the basis of pre-clinical studies on mdx mice [105,106]. In order to enroll a highly chance cohort of responsive patients, on-going clinical trials with Givinostat are selectively recruiting ambulant dystrophic boys (that correspond to the early stages of DMD [119]).

The stage-dependent activity of HDACi arises two crucial emergencies for current clinical studies:

I) identify specific biomarkers to predict and monitor HDACi responsiveness;

II) develop novel cocktail therapies to extend HDACi at late stages of DMD.

This project holds the potential to achieve both of them.

To date, physicians had to rely on functional tests or muscle biopsy to monitor DMD progression and the efficacy of HDACis treatment, as no reliable marker in body fluids as yet been identified. Our acetylome profiling revealed a completely different pattern of histone acetylation at different stages of DMD, and in response to HDACi. By dissecting highly significant differential peaks among samples, we were able to identify the Epi-Signature that characterize HDACi activity at early and late stages of DMD in FAPs and mapped their characteristic genomic loci. This technology can pioneer an innovative diagnostic and prognostic device able to predict the responsiveness to HDACis from dystrophic patients' biopsies. Furthermore, even if most of the studies regarding HDACis efficacy are focused on their role in FAPs, it is possible that they may also target other cellular populations, such as circulating blood cells. If HDACis would assign an Epi-signature of responsiveness and resistance to circulating blood cells, we could be able to predict the efficacy to HDACis and follow the progression of the pathology from a simple blood test. Further studies would be required though.

Moreover, our study unveiled dramatic changes of FAP chromatin during DMD progression that affect their responsiveness to HDACi. The altered epigenetic landscape of old FAPs suggest that combined epigenetic treatments could synergize to boost and extend HDACi efficacy at later stages of DMD. For instance, we speculate that the striking loss of AcH3K27 in old FAPs could match with an increasing H3K27me3, prospecting therapeutic strategies with combined PRC2 and HDAC inhibitors.
Further studies will develop these exciting perspectives. Of note, devising pharmacological cocktail strategies represents the most immediate and suitable approach to counteract DMD progression in the current generation of dystrophic patients, waiting for more definitive genetic approach.

Moreover, in contrast with other strategies to treat DMD, such as Exon skipping [96], regenerative pharmacology is potentially applicable to any genetic sub-type of DMD and other Muscular Dystrophies.

The Epigenetic modifications that differentiate the effect of TSA in early or late stages of DMD have a fundamental effect on their transcriptome, and how HDACis are able to modulate key biological functions for muscle regeneration. In this work we propose a model of biological function prediction that is very consistent with the presented results, and with already published data from the literature. For example, we find the categories of "Cell to Cell interactions" and "Formation of muscle" to be Promoted or "Adipogenesis of Cells" to be inhibited, and their modulation is perfectly consistent with the literature [23,62,101].
This analysis represented a clear reference point that we followed during the development of the project. By trailing it, and using supporting bio-informatic analysis, we discovered the modulation of several biological functions that were never studied in the context of HDACis treatment. Here we demonstrated by a combination of histological immunofluorescence, cytofluorimetric analysis and ex-vivo cell culture, that HDACis activates a long-lasting cell cycle in FAPs from 1.5 months old mdx animals, and we suggest that this represent an effort in synchronizing efficient muscle regeneration. Moreover, it has also been demonstrated that the S-phase entry is required for epigenetic modifications to occur [120]. In this context, a longer cell cycle would mean a longer S-phase, and thus more time to change the chromatin landscape of FAPs.
Our data also show that TSA promotes the migration of responsive, dystrophic FAPs within the muscular tissue. DMD, as any other chronic muscle wasting diseases, is a concert of asynchronous foci of muscle degeneration and regeneration [99].
With this work, we are proposing a model of "Enhanced Muscular Regeneration" in which HDACi activates, and keeps ready, a high

number of resident FAPs in dystrophic muscle to respond to environmental cues and quickly migrate to the site of injury to promote MuSCs mediated muscle regeneration. Furthermore, we do not exclude that non-resident progenitors may also migrate from the blood stream to help the muscular regeneration, as the extravasation process is predicted to be activated in responsive FAPs post-TSA treatment. Further investigation would be needed to validate this hypothesis though. In un-responsive mdx mice, represented by late stages of DMD, HDACis are predicted to have a complete opposite effect on mdx FAPs. In this study we have demonstrated *in vivo* and *ex vivo* that HDACi at this stage are not anymore able to promote the cell cycle progression, nor cell activation or cell migration. In particular we demonstrated that DMD progression alters in a profound way both, the epigenetic and the muscular environment. In fact, by plating late stages mdx FAPs *ex vivo* we observed a reduction of cell survival and cell proliferation. Especially after in-vivo TSA treatment.

Furthermore, our *in vivo* analysis revealed that the environment plays an important role on how mdx FAPs behave in response to TSA, as by transplanting un-responsive HDACis treated mdx FAPs in 1.5 months old dystrophic muscles, we were able to partially recover the effect of TSA in promoting both migration and cell survival.

The information provided by this study crucially expands the knowledge about the therapeutic approach of HDACis for the treatment of DMD. It characterizes the differential role of HDACis during the progression of the pathology, linking the epigenetics with the transcriptomics and translating the latter in the modulation of actual biological functions, fundamental for muscular regeneration.

5 Materials and Methods

5.1 Animals and in vivo treatment

Mice were bred, handled and maintained according to the standard animal facility procedures and the internal Animal Research Ethical Committee according to the Italian Ministry of Health approved all experimental protocols and the ethic committee of the Fondazione Santa Lucia (FSL) approved protocols.
C57Bl6 mdx mice were purchased from Jackson Laboratories.
Animals were used at the specified age and treated for the indicated periods with daily intra peritoneal injections of Trichostatin A, TSA (0.6 mg/kg/day; #T8552, Sigma), dissolved in in phospate-saline solution or in phospate-saline alone as vehicle control (CTR).
20 mg/Kg EdU (Click-IT Plus EdU; Invitrogen) were injected by IP 24 hours before sacrifice.
20 ul of FACs sorted FAPs stained with PKH-67 (#MINI-67, Sigma) following the manufacture protocol were injected in the proximal part of the gastrocnemius from the foot-paw of MDX mice at the concentration of 5000 cells/ul.

5.2 Histology

The Tibialis anterior muscles were snap frozen in liquid nitrogen-cooled isopentane and then cut transversally with a thickness of 8 μm.

5.3 Isolation of FAPs and Satellite cells (MuSCs)

FAP cells were isolated as TER119-/CD45-/CD31-/ a7INTEGRIN-/SCA-1+ cells, MuSCs were isolated as TER119-/CD45-/CD31-/a7INTEGRIN+/SCA-1- cells.
Briefly, hind limb muscles for each mouse were minced and put into a 15 mL tube containing 4 mL of HBSS (#24020-091,GIBCO) BSA (0.2%, #A7030, Sigma) and 10 Units/ml Penicillin and 10 μg/ml streptomycin (P/S), 2 mg/ml Collagenase A (#10103586001, Roche), 2.4U/ml Dispase II (#04942078001, Roche), DNaseI 10

mg/ml (#11284932001, Roche) at 37°C under gentle agitation for approximately 1hr and 30 min.
The supernatants were filtered through a 100um, 70um and 40um cell strainers (#08-771-19, #08-771-2, #08-771-1, BD Falcon). Cells were spun for 15 min at 300 g at 4°C, the pellets were re-suspended in 0.5 mL of HBSS 1x containing DNase I and incubated with antibodies on ice for 30 min. The following antibodies were used: CD45-eFluor 450 (1/50, #48-0451-82, Leukocyte Common Antigen, Ly-5, eBiosciences), CD31- eFluor 450 (1/50, PECAM-1, #48-0311-82, eBioscience), TER- 119-eFluor 450 (1/50, clone TER-119, #48-5921-82, eBiosciences), Sca1-FITC (1/50, Ly-6A/E FITC, clone D7, #11- 5981-82, eBioscience), Itga7-649 (1/500, AbLab #67-0010-01), rat anti-SCA-1 APC fire750 (1:100, #108145, biolegend). HBSS was added and cells were spun for 5 min at 300 g at 40C to stop the reaction. The cells were re-suspended in HBSS containing 1% DNaseI and were isolated based on size, granulosity and fluorophores levels using a FACS MoFlo HS Cell Sorter Dako Cytomation (BD) and analyzed using FlowJo.
Example of the FACS gates:

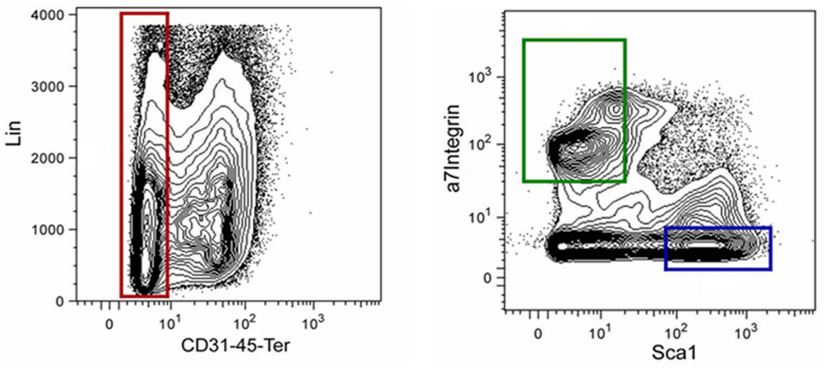

5.4 Sample preparation for the cytofluorimetric analysis

Similarly to the protocol of FAC sorting: hind limb muscles were minced and digested in HBSS (Gibco) containing 2 ug/mL Collagenase A (Roche), 2.4 U/mL Dispase I (Roche), 10 ng/mL DNase I (Roche), 0.4 mM CaCl2 and 5mM MgCl2 for 90 min at 37° C. Cells were then filtered through 100um, 70um and 40um filters. Cells were stained with primary antibodies (Same as FACs) for 30 min on ice. Cells were finally washed and resuspended in HBSS containing 0.2% (w/v) BSA and 1% (v/v) Penicillin-Streptomycin.
Then cells were fixed in 4% Formaldehyde and washed 2 times in PBs. For the EdU experiment, the cells were stained for EdU following the manufacturer protocol. Cells were analyzed at the cytofluorimeter "CytoFLEX" (Beckman Coulter Life Sciences). In detail, the single cells were defined using the physical parameters (FSC and SSC), FAPs, MuSCs and Lin+ cells were defined as explained in the FACs paragraph. Both the EdU and PkH-67 positivity were gated against the laser v525.

Example of a gate for EdU positivity:

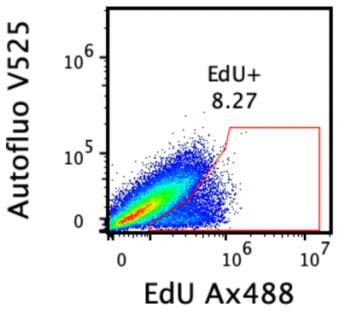

Example of a gate for PkH-67 positivity:

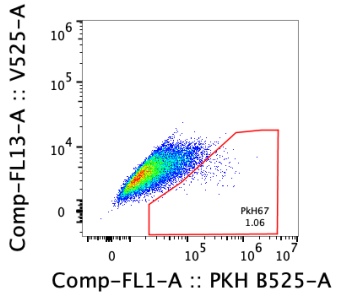

5.5 Culture conditions of FAPs

Freshly sorted cells were plated in BIOAMF-2 complete medium (ATGC), 1% Penicillin-Streptomycin (#15140, GIBCO), as a growth medium (GM). For the EdU experiment, 3 x 10^4 FAPs on 24 multi-wells well. For the Migration experiment, 5 x 10^3 FAPs on 96 multi-wells well.

For TSA *in vitro* treatment, cells were treated with 50nM TSA in GM. For the Edu experiment, the Media was changed right before the incubation with EdU. For the Wound Healing Assay, the media was changed right before inflicting the wound to the cell layer.

For the EdU in vitro Treatment, the EdU molecule was used at the concentration suggested by the manufacturer.

5.6 Immunofluorescence

For immunofluorescence analysis, cryo-sections and cells were fixed in 4% PFA for 10 min and permeabilized with 100% cold acetone (#32201, Sigma) for 6 min at -20°C or 100% cold Methanol (#32213, Sigma) for 6 min at -20° or with 0,25% Triton for 15 min at RT. Muscle sections were blocked for 1h with a solution containing 4% BSA (#A7030, Sigma) in PBS. The primary antibodies incubation was performed O.N. at 4°C and then the antibody binding specificity was revealed using secondary antibodies coupled to Alexa Fluor 488, 594, or 647 (Invitrogen). Sections were incubated with DAPI in PBS for 5 minutes for nuclear staining, washed in PBS, and mounted with glycerol 3:1 in PBS. The primary antibody used for immunofluorescences is: rabbit anti-Laminin (1/400, #L9393, Sigma). For the EdU experiment, the staining was perfomed following the manufacturer protocol.

5.7 RT-PCR

Total RNA was extracted with Trizol, and 0,5-1 ug were retrotranscribed using the Taqman reverse transcription kit (Applied Biosystems). Real time quantitative PCR was performed

to analyze relative gene expression levels using SYBR Green Master mix (Applied Biosystems) following manufacturer indications. Relative expression values were normalized to the housekeeping gene GAPDH.

GAPDH:
Fwd: CACCATCTTCCAGGAGCGAG
Rev: CCTTCTCCATGGTGGTGAAGAC

Ki-67
Fwd: TCACCTGGGTCACCATCAAGC
Rev: TCAATACTCCTTCCAAACAGGCA

5.8 Sample preparation for sequencing

5.8.1 RNA-sequencing

For RNA-sequencing sample preparation, MuSCs and FAPs were freshly isolated by FACS from 6 C57Bl6J mdx male mice for experimental point (1.5 months and 12 months old treated with TSA or its vehicle of control for 15 days). RNA was collected using Trizol) reagent (#T9424, Sigma). About 100 ng/ul of total RNA was sent in duplicate to IGA (Istituto di Genomica Applicata, Udine) for RNA sequencing using Illumina TruSeq Stranded Total RNA kit Ribo-Zero GOLD on Illumina Hiseq2500 platform.

5.8.2 ChIP-sequencing

For ChIP-sequencing sample preparation, MuSCs and FAPs were freshly isolated by FACS from 10 C57Bl6J mdx male mice for experimental point (1.5 and 12 month old treated with TSA or its vehicle of control for 15 days). The cells were fixed in 3.7% PFA for 12 Minutes, then glycine was used to stop the reaction, the cells were washed with PBS and protease inhibitors. The pellet was frozen at -80 °C overnight. The cells were resuspended in Cell Lysis buffer (10mM Tris pH 8.0); 10 mM NaCl; 0.2% NP40 and protease inhibitors), to lyse the cells. After a centrifugation steps,

the nuclei were lysed with the Nuclei Lysis Buffer (50Mm tris HCL pH 8.1; 10mM EDTA; 1%SDS and protease inhibitors) and the chromatin was sonicated to an average length of about 200bp (4 cycles: 30 sec ON, 45sec OFF for 5 minutes). Chromatin was diluted 1:10 in IP Dilution buffer (0.01%SDS; 1.1% TritonX 100; 1.2mM EDTA; 16.7mM TrisHCl pH 8.1; 167mM NaCl). Chromatin was cleared with Magnetic Beads, and then 100 ug were immune-precipitated ON at +4°C with the antibodies (10 ul for AcH3K9/14 and AcH3K27). The Chromatin was washed twice with Low Salt buffer (0.1% SDS, 1% Triton, 2mM EDTA; 20mM Tris pH8, 150mM NaCl), High Salt buffer (0.1% SDS, 1% Triton, 2mM EDTA; 20mM Tris pH8, 500mM NaCl), Lithium Buffer (0.25M LiCl; 1%NP40; 1% deoxycholate; 1mM EDTA; 10mM Trish pH8) and TE 1X. Then the antibody was eluted in IP Elution Buffer (1%SDS; 1mM EDTA; 10mM Trish pH8) at 65°C for 15 minutes and the crosslink was reversed by ON incubation at 65°C. The proteins were enzymatically digested in proteinase K for 2 Hours at 37°C and the DNA was extracted in phenol chloroform.
ChIP-seq samples were sent to IGA (Istituto di Genomica Applicata, Udine) for ChIP-sequencing on Illumina Hiseq2500 platform.

5.9 Statistical analysis

The number of independent experimental replications and precision measures are reported in the figure legends (n, mean ± sem or n, mean ± sd). Comparisons between two groups were made using the Student's t-test assuming a two-tailed distribution, with significance being defined as */†/❋ $p<0.05$; **/††/❋❋ $p<0.01$; ***/†††/❋❋❋ $p<0.001$; ****/††††/❋❋❋❋ $p<0.0001$. Comparisons between three or more groups were made using one-way or two way Anova test (depending on the number of factors taken into account in the analysis), with significance being defined as # $p<0.05$; ## $p<0.01$; ### $p<0.001$; ### $p<0.0001$.

5.10 Data and Software availability

The cells positive for the stainings described in the text were quantified using (https://imagej.nih.gov/ij/download.html), the ImageJ software. FACS profile analysis of Lin, MuSCs and FAPs were performed using Flowjo software (https://www.flowjo.com). The Box-plots, Histograms and Heatmaps were generated in PRISM 8.

5.11 Bioinformatic Analysis

5.11.1 RNA-seq analysis

The RNA sequencing analysis was performed Mapping more than 20 millions of reads for each sample to the Mus Musculus GRCm38.78 genome using TopHat 2.0.9. Read count was performed with HTSeq-0.6.1p1. Mapped reads were analyzed with R-studio (R version 3.5.2) using DESeq2 to obtain normalized RPKM, P- Value, P-adjusted and log2fold changes values. Genes were considered differentially expressed if the P-adjusted value was < 0.1. The Heatmap with the Z-score was generated with "Pheatmap". The z-score was calculated as follows:

```
Zscore=function(x){
  y=x
  for(i in 1:nrow(x)){
    for(j in 1:ncol(x)){
      y[i,j]=(x[i,j]-mean(x[i,]))/sd(x[i,])
    }
  }
  return(y)}
```

The volcano plot were generated with DESeq2. The PCA was generated in R-studio taking into account the 1000 significantly most modulated genes with the package "PCAExplorer". The gene

ontology for the PC-1 and PC-2 was also generated in PCAExplorer.

5.11.2 ChIP-seq analysis

ChIP-seq reads were aligned to the genome using the bowtie-0.12.7 alignment software. Duplicated reads were removed using samtools1.3. Regions of AcH3K9/14 and AcH3K27 occupancy were determined using macs2 with a FDR < 0.001 and an ExtSize of 147. Input DNA of each sample was used as the control of the Peak Calling. BlackList regions of the murine genome (ENCFF547MET.bed) were excluded using the software bedtools. macs 2 significant peaks were further filtered using a threshold of macs_score > 100.

5.11.3 ChIP-seq visualization

ChIP-seq bam files were filtered in and out the promoters (Described as -1500/+500) with bedtools and then compared against each other using NGSplot (https://github.com/shenlab-sinai/ngsplot) . ChIP-seq bed files for every sample of AcH3 and AcH3K27 were merged to form a single bed file for each histone modification. The genomic distribution was then analyses with ChIP-Seeker.

5.11.4 Differential Peak calling

The BedSum file, containing the regions to compare for the differential peak calling, were generated merging and sorting the two bed files of the samples of interest using bedtools. The same bed files were processed in tagDir using the Homer makeTagDirectory command.
Differentially acetylated regions were generated comparing the BedSum file to either tagDir using Homer getDifferentialPeaks command with a fold change of 2.

5.11.5 Motif discovery

Differentially acetylated peaks were analyzed for known motif enrichment using Homer “findMotifsGenome.pl” with default

parameters. In R-studio the motifs were filtered against the RNA-seq data. In particular only Motifs for genes that had at least 100 "reads count normalized" across our samples were taken into account. Different motifs for the same factors were kept for completeness. The heatmap was generated by using Graphpad prism 8.0. Only motifs for gene families composed of at least 2 members are displayed.

5.11.6 De-Novo and Hyper-Acetylated peaks

Homer differential peaks were intersected with the bed file of the contrast of control using BedTools with the options -wa -u for Hyper-Acetylated peaks and the option -v for De-Novo peaks.

5.11.7 Differential peaks overlap

Homer differential peaks were analyzed for overlapping regions using the Intervene tool with default parameters. The matrix of overlaps was uploaded in the intervene shiny app (https://asntech.shinyapps.io/intervene/) and the Upset graph was generated.

5.11.8 Integration of ChIP peaks with RNAsq

The bed files generated from Homer or Intervene were intersected with a bed file containing all the promoter locations of mm10 using BedTools intersect. Peaks on the promoters were filtered in R 3.5.2 with transcripts significantly modulated (Padj < 0.1) by RNA-seq. The heatmap was generated by using Graphpad prism 8.0.

5.11.9 Putative enhancer-promoter interaction

The bed files generated from Homer differential analysis were intersected with a bed file containing all the promoter locations of mm10 using BedTools intersect -v. Peaks outside the promoter were uploaded in GREAT (http://great.stanford.edu/public/html/) and the results were downloaded as .csv tables. The results were further analyzed and integrated with the RNA-seq in R 3.5.2. The

histograms were generated in Graphpad prism 8.0. The venn diagram was generated in (http://eulerr.co).

5.11.10Biological Processes prediction analysis.

Whole RNA-seq comparisons generated by DESEq2, Hyper-acetylated peaks and Hypo-acetylated peaks for AcH3k9/14 and K27 were integrated with, respectively, up-regulated genes and down-regulated genes by RNA-seq in R 3.5.2 and uploaded in IPA. Genes with Padj < 0.1 were used for every core-analysis. The core analysis were compared via the "comparison analysis" tools. The "Disease and biofunctions" table of the comparison analysis was downloaded as .txt file and further analyzed in R 3.5.2. The results were filtered to have the most significative modulated cluster of biological functions across the datasets. The clusters were manually curated to only display biological function of relevance and the results were showed as an Heatmap generated in GraphPad prism 8.0. Images on the right were downloaded from (https://app.biorender.com).

5.11.11IPA Custom Network

From the core analysis of Young TSA FAPs with Padj < 0.1, we selected the genes that were predicted to be activating either the "Activation of cells" or the "Cell Cycle Progression" and created a new custom pathway. We then connected in un-biased way the different genes with each other using the relationships "Activation" or "Inhibition" and then connected "Activation of cells" or the "Cell Cycle Progression" with all of them to see the overlap of interactions. For a better presentation, the network was rendered in the IPA "PathDesigner".

6 References

1. Frontera, W. R. & Ochala, J. Skeletal Muscle: A Brief Review of Structure and Function. *Behav. Genet.* **45**, 183–195 (2015).

2. Yusuf, F. & Brand-Saberi, B. Myogenesis and muscle regeneration. *Histochemistry and Cell Biology* (2012). doi:10.1007/s00418-012-0972-x

3. Chargé, S. B. P. & Rudnicki, M. A. Cellular and Molecular Regulation of Muscle Regeneration. *Physiol. Rev.* **84**, 209–238 (2004).

4. S. Hikida, R. Aging Changes in Satellite Cells and Their Functions. *Curr. Aging Sci.* (2012). doi:10.2174/1874609811104030279

5. MacAluso, F. & Myburgh, K. H. Current evidence that exercise can increase the number of adult stem cells. *J. Muscle Res. Cell Motil.* (2012). doi:10.1007/s10974-012-9302-0

6. Chang, N. C. & Rudnicki, M. A. Satellite Cells: The Architects of Skeletal Muscle. in *Current Topics in Developmental Biology* (2014). doi:10.1016/B978-0-12-416022-4.00006-8

7. Comai, G. & Tajbakhsh, S. Molecular and cellular regulation of skeletal myogenesis. in *Current Topics in Developmental Biology* (2014). doi:10.1016/B978-0-12-405943-6.00001-4

8. Pawlikowski, B., Pulliam, C., Betta, N. D., Kardon, G. & Olwin, B. B. Pervasive satellite cell contribution to uninjured adult muscle fibers. *Skelet. Muscle* (2015). doi:10.1186/s13395-015-0067-1

9. Robinson, D. C. L. & Dilworth, F. J. Epigenetic Regulation of Adult Myogenesis. in *Current Topics in Developmental Biology* (2018). doi:10.1016/bs.ctdb.2017.08.002

10. Bareja, A. *et al.* Human and mouse skeletal muscle stem cells: Convergent and divergent mechanisms of myogenesis. *PLoS One* (2014). doi:10.1371/journal.pone.0090398

11. Konigsberg, U. R., Lipton, B. H. & Konigsberg, I. R. The regenerative response of single mature muscle fibers isolated in vitro. *Dev. Biol.* (1975). doi:10.1016/0012-1606(75)90065-2

12. Bischoff, R. Regeneration of single skeletal muscle fibers in vitro. *Anat. Rec.* (1975). doi:10.1002/ar.1091820207

13. Kibler, W. Ben & Armstrong, R. B. Initial events in exercise-induced muscular injury. *Med. Sci. Sports Exerc.* (1990).

14. Lawlor, M. A. & Rotwein, P. Insulin-Like Growth Factor-Mediated Muscle Cell Survival: Central Roles for Akt and Cyclin-Dependent Kinase Inhibitor p21. *Mol. Cell. Biol.* (2000). doi:10.1128/mcb.20.23.8983-8995.2000

15. Tidball, J. G. Inflammatory processes in muscle injury and repair. *American Journal of Physiology - Regulatory Integrative and Comparative Physiology* (2005). doi:10.1152/ajpregu.00454.2004

16. McClung, J. M., Davis, J. M. & Carson, J. A. Ovarian hormone status and skeletal muscle inflammation during recovery from disuse in rats. *Exp. Physiol.* (2007). doi:10.1113/expphysiol.2006.035071

17. Deng, B., Wehling-Henricks, M., Villalta, S. A., Wang, Y. & Tidball, J. G. IL-10 Triggers Changes in Macrophage Phenotype That Promote Muscle Growth and Regeneration.

J. Immunol. (2012). doi:10.4049/jimmunol.1103180

18. Tedesco, F. S., Moyle, L. A. & Perdiguero, E. Muscle interstitial cells: A brief field guide to non-satellite cell populations in skeletal muscle. in *Methods in Molecular Biology* (2017). doi:10.1007/978-1-4939-6771-1_7

19. Joe, A. W. B. *et al.* Muscle injury activates resident fibro/adipogenic progenitors that facilitate myogenesis. *Nat. Cell Biol.* **12**, 153–163 (2010).

20. Uezumi, A., Fukada, S. I., Yamamoto, N., Takeda, S. & Tsuchida, K. Mesenchymal progenitors distinct from satellite cells contribute to ectopic fat cell formation in skeletal muscle. *Nat. Cell Biol.* **12**, 143–152 (2010).

21. Lemos, D. R. *et al.* Nilotinib reduces muscle fibrosis in chronic muscle injury by promoting TNF-mediated apoptosis of fibro/adipogenic progenitors. *Nat. Med.* (2015). doi:10.1038/nm.3869

22. Uezumi, A. *et al.* Fibrosis and adipogenesis originate from a common mesenchymal progenitor in skeletal muscle. *J. Cell Sci.* **124**, 3654–3664 (2011).

23. Saccone, V. *et al.* HDAC-regulated myomiRs control BAF60 variant exchange and direct the functional phenotype of fibro-adipogenic progenitors in dystrophic muscles. *Genes Dev.* (2014). doi:10.1101/gad.234468.113

24. Heredia, J. E. *et al.* Type 2 innate signals stimulate fibro/adipogenic progenitors to facilitate muscle regeneration. *Cell* (2013). doi:10.1016/j.cell.2013.02.053

25. Villalta, S. A., Nguyen, H. X., Deng, B., Gotoh, T. & Tidbal, J. G. Shifts in macrophage phenotypes and macrophage competition for arginine metabolism affect the severity of muscle pathology in muscular dystrophy. *Hum.*

Mol. Genet. (2009). doi:10.1093/hmg/ddn376

26. Waddington, C. H. The epigenotype. 1942. *Int. J. Epidemiol.* (2012). doi:10.1093/ije/dyr184

27. Waddington, C. H. Canalization of development and the inheritance of acquired characters. *Nature* (1942). doi:10.1038/150563a0

28. Allis, C. D. & Jenuwein, T. The molecular hallmarks of epigenetic control. *Nat. Rev. Genet.* **17**, 487–500 (2016).

29. Sterner, D. E. & Berger, S. L. Acetylation of Histones and Transcription-Related Factors. *Microbiol. Mol. Biol. Rev.* **64**, 435–459 (2000).

30. Luger, K., Mäder, A. W., Richmond, R. K., Sargent, D. F. & Richmond, T. J. Crystal structure of the nucleosome core particle at 2.8 Å resolution. *Nature* (1997). doi:10.1038/38444

31. Lawrence, M., Daujat, S. & Schneider, R. Lateral Thinking: How Histone Modifications Regulate Gene Expression. *Trends Genet.* **32**, 42–56 (2016).

32. Heitz, E. Das Heterochromatin der Moose. *Jahrbücher für wissenschaftliche Bot.* (1928). doi:10.5244/C.2.23

33. Klemm, S. L., Shipony, Z. & Greenleaf, W. J. Chromatin accessibility and the regulatory epigenome. *Nat. Rev. Genet.* **20**, 207–220 (2019).

34. Bannister, A. J. & Kouzarides, T. Regulation of chromatin by histone modifications. *Cell Res.* **21**, 381–395 (2011).

35. Long, H. K., Prescott, S. L. & Wysocka, J. Ever-Changing Landscapes: Transcriptional Enhancers in Development and Evolution. *Cell* (2016). doi:10.1016/j.cell.2016.09.018

36. Haberle, V. & Stark, A. Eukaryotic core promoters and the functional basis of transcription initiation. *Nature Reviews Molecular Cell Biology* (2018). doi:10.1038/s41580-018-0028-8

37. Schoenfelder, S. & Fraser, P. Long-range enhancer–promoter contacts in gene expression control. *Nat. Rev. Genet.* (2019). doi:10.1038/s41576-019-0128-0

38. Mifsud, B. *et al.* Mapping long-range promoter contacts in human cells with high-resolution capture Hi-C. *Nat. Genet.* (2015). doi:10.1038/ng.3286

39. Zentner, G. E., Tesar, P. J. & Scacheri, P. C. Epigenetic signatures distinguish multiple classes of enhancers with distinct cellular functions. *Genome Res.* (2011). doi:10.1101/gr.122382.111

40. Chen, T. & Dent, S. Y. R. Chromatin modifiers and remodellers: regulators of cellular differentiation. *Nat. Rev. Genet.* **15**, 93–106 (2014).

41. Hyun, K., Jeon, J., Park, K. & Kim, J. Writing, erasing and reading histone lysine methylations. *Exp. Mol. Med.* **49**, (2017).

42. Wang, Z. *et al.* Combinatorial patterns of histone acetylations and methylations in the human genome. *Nat. Genet.* (2008). doi:10.1038/ng.154

43. Kouzarides, T. Chromatin Modifications and Their Function. *Cell* (2007). doi:10.1016/j.cell.2007.02.005

44. Mujtaba, S., Zeng, L. & Zhou, M. M. Structure and acetyl-lysine recognition of the bromodomain. *Oncogene* (2007). doi:10.1038/sj.onc.1210618

45. Hassan, A. H. *et al.* Function and selectivity of

bromodomains in anchoring chromatin-modifying complexes to promoter nucleosomes. *Cell* (2002). doi:10.1016/S0092-8674(02)01005-X

46. Black, J. C., Van Rechem, C. & Whetstine, J. R. Histone Lysine Methylation Dynamics: Establishment, Regulation, and Biological Impact. *Molecular Cell* (2012). doi:10.1016/j.molcel.2012.11.006

47. Vastenhouw, N. L. & Schier, A. F. Bivalent histone modifications in early embryogenesis. *Current Opinion in Cell Biology* (2012). doi:10.1016/j.ceb.2012.03.009

48. Barski, A. *et al.* High-Resolution Profiling of Histone Methylations in the Human Genome. *Cell* (2007). doi:10.1016/j.cell.2007.05.009

49. ALLFREY, V. G., FAULKNER, R. & MIRSKY, A. E. ACETYLATION AND METHYLATION OF HISTONES AND THEIR POSSIBLE ROLE IN THE. *Proc. Natl. Acad. Sci. United States* (1964). doi:10.1073/pnas.51.5.786

50. Nasir Javaid and Sangdun Choi. Acetylation- and Methylation-Related Epigenetic Proteins in the Context of Their Targets. *Genes (Basel).* **8**, 196 (2017).

51. Marmorstein, R. & Zhou, M. M. Writers and readers of histone acetylation: Structure, mechanism, and inhibition. *Cold Spring Harb. Perspect. Biol.* **6**, 1–25 (2014).

52. Yang, X. J. & Seto, E. HATs and HDACs: From structure, function and regulation to novel strategies for therapy and prevention. *Oncogene* (2007). doi:10.1038/sj.onc.1210599

53. Hodawadekar, S. C. & Marmorstein, R. Chemistry of acetyl transfer by histone modifying enzymes: Structure, mechanism and implications for effector design. *Oncogene* (2007). doi:10.1038/sj.onc.1210619

54. Barnes, C. E., English, D. M. & Cowley, S. M. Acetylation and Co: An expanding repertoire of histone acylations regulates chromatin and transcription. *Essays Biochem.* **63**, 97–107 (2019).

55. Luebben, W. R., Sharma, N. & Nyborg, J. K. Nucleosome eviction and activated transcription require p300 acetylation of histone H3 lysine 14. *Proc. Natl. Acad. Sci. U. S. A.* (2010). doi:10.1073/pnas.1009650107

56. Gates, L. A. *et al.* Acetylation on histone H3 lysine 9 mediates a switch from transcription initiation to elongation. *J. Biol. Chem.* (2017). doi:10.1074/jbc.M117.802074

57. Creyghton, M. P. *et al.* Histone H3K27ac separates active from poised enhancers and predicts developmental state. *Proc. Natl. Acad. Sci. U. S. A.* (2010). doi:10.1073/pnas.1016071107

58. Visel, A. *et al.* ChIP-seq accurately predicts tissue-specific activity of enhancers. *Nature* (2009). doi:10.1038/nature07730

59. Pradeepa, M. M. *et al.* Histone H3 globular domain acetylation identifies a new class of enhancers. *Nat. Genet.* (2016). doi:10.1038/ng.3550

60. Taylor, G. C. A., Eskeland, R., Hekimoglu-Balkan, B., Pradeepa, M. M. & Bickmore, W. A. H4K16 acetylation marks active genes and enhancers of embryonic stem cells, but does not alter chromatin compaction. *Genome Res.* (2013). doi:10.1101/gr.155028.113

61. Buggy, J. J. *et al.* Cloning and characterization of a novel human histone deacetylase, HDAC8. *Biochem. J.* (2000). doi:10.1042/0264-6021:3500199

62. Dokmanovic, M., Clarke, C. & Marks, P. A. Histone

deacetylase inhibitors: Overview and perspectives. *Mol. Cancer Res.* **5**, 981–989 (2007).

63. Singh, K. & Dilworth, F. J. Differential modulation of cell cycle progression distinguishes members of the myogenic regulatory factor family of transcription factors. *FEBS Journal* (2013). doi:10.1111/febs.12188

64. Liu, Y., Chu, A., Chakroun, I., Islam, U. & Blais, A. Cooperation between myogenic regulatory factors and SIX family transcription factors is important for myoblast differentiation. *Nucleic Acids Res.* (2010). doi:10.1093/nar/gkq585

65. Bracken, A. P., Dietrich, N., Pasini, D., Hansen, K. H. & Helin, K. Genome-wide mapping of polycomb target genes unravels their roles in cell fate transitions. *Genes Dev.* (2006). doi:10.1101/gad.381706

66. Caretti, G., Di Padova, M., Micales, B., Lyons, G. E. & Sartorelli, V. The Polycomb Ezh2 methyltransferase regulates muscle gene expression and skeletal muscle differentiation. *Genes Dev.* (2004). doi:10.1101/gad.1241904

67. Boonsanay, V. *et al.* Regulation of Skeletal Muscle Stem Cell Quiescence by Suv4-20h1-Dependent Facultative Heterochromatin Formation. *Cell Stem Cell* (2016). doi:10.1016/j.stem.2015.11.002

68. Kawabe, Y. I., Wang, Y. X., McKinnell, I. W., Bedford, M. T. & Rudnicki, M. A. Carm1 regulates Pax7 transcriptional activity through MLL1/2 recruitment during asymmetric satellite stem cell divisions. *Cell Stem Cell* (2012). doi:10.1016/j.stem.2012.07.001

69. McKinnell, I. W. *et al.* Pax7 activates myogenic genes by

recruitment of a histone methyltransferase complex. *Nat. Cell Biol.* (2008). doi:10.1038/ncb1671

70. Fritsch, L. *et al.* A Subset of the Histone H3 Lysine 9 Methyltransferases Suv39h1, G9a, GLP, and SETDB1 Participate in a Multimeric Complex. *Mol. Cell* (2010). doi:10.1016/j.molcel.2009.12.017

71. Gillespie, M. A. *et al.* p38-γ-dependent gene silencing restricts entry into the myogenic differentiation program. *J. Cell Biol.* (2009). doi:10.1083/jcb.200907037

72. Liu, L. *et al.* Chromatin Modifications as Determinants of Muscle Stem Cell Quiescence and Chronological Aging. *Cell Rep.* (2013). doi:10.1016/j.celrep.2013.05.043

73. Palacios, D. & Puri, P. L. The epigenetic network regulating muscle development and regeneration. *Journal of Cellular Physiology* (2006). doi:10.1002/jcp.20489

74. Rao, P. K., Kumar, R. M., Farkhondeh, M., Baskerville, S. & Lodish, H. F. Myogenic factors that regulate expression of muscle-specific microRNAs. *Proc. Natl. Acad. Sci. U. S. A.* (2006). doi:10.1073/pnas.0602831103

75. Puri, P. L. *et al.* Class I histone deacetylases sequentially interact with MyoD and pRb during skeletal myogenesis. *Mol. Cell* (2001). doi:10.1016/S1097-2765(01)00373-2

76. Mal, A., Sturniolo, M., Schiltz, R. L., Ghosh, M. K. & Harter, M. L. A role for histone deacetylase HDAC1 in modulating the transcriptional activity of MyoD: Inhibition of the myogenic program. *EMBO J.* (2001). doi:10.1093/emboj/20.7.1739

77. McKinsey, T. A., Zhang, C. L. & Olson, E. N. Activation of the myocyte enhancer factor-2 transcription factor by calcium/calmodulin-dependent protein kinase-stimulated

binding of 14-3-3 to histone deacetylase 5. *Proc. Natl. Acad. Sci. U. S. A.* (2000). doi:10.1073/pnas.260501497

78. Guasconi, V. & Puri, P. L. Chromatin: the interface between extrinsic cues and the epigenetic regulation of muscle regeneration. *Trends in Cell Biology* (2009). doi:10.1016/j.tcb.2009.03.002

79. Sartorelli, V. *et al.* Acetylation of MyoD directed by PCAF is necessary for the execution of the muscle program. *Mol. Cell* (1999). doi:10.1016/S1097-2765(00)80383-4

80. Ma, K., Chan, J. K. L., Zhu, G. & Wu, Z. Myocyte Enhancer Factor 2 Acetylation by p300 Enhances Its DNA Binding Activity, Transcriptional Activity, and Myogenic Differentiation. *Mol. Cell. Biol.* (2005). doi:10.1128/mcb.25.9.3575-3582.2005

81. Angelelli, C. *et al.* Differentiation-dependent lysine 4 acetylation enhances MEF2C binding to DNA in skeletal muscle cells. *Nucleic Acids Res.* (2008). doi:10.1093/nar/gkm1114

82. Lan, F. *et al.* A histone H3 lysine 27 demethylase regulates animal posterior development. *Nature* (2007). doi:10.1038/nature06192

83. Seenundun, S. *et al.* UTX mediates demethylation of H3K27me3 at muscle-specific genes during myogenesis. *EMBO J.* (2010). doi:10.1038/emboj.2010.37

84. Wang, A. H. *et al.* The histone chaperone Spt6 coordinates histone H3K27 demethylation and myogenesis. *EMBO J.* (2013). doi:10.1038/emboj.2013.54

85. Nielsen, S. J. *et al.* Rb targets histone H3 methylation and HP1 to promoters. *Nature* (2001). doi:10.1038/35087620

86. Hamed, M., Khilji, S., Chen, J. & Li, Q. Stepwise acetyltransferase association and histone acetylation at the Myod1 locus during myogenic differentiation. *Sci. Rep.* (2013). doi:10.1038/srep02390

87. Choi, J. *et al.* Histone demethylase LSD1 is required to induce skeletal muscle differentiation by regulating myogenic factors. *Biochem. Biophys. Res. Commun.* (2010). doi:10.1016/j.bbrc.2010.09.014

88. Asp, P. *et al.* Genome-wide remodeling of the epigenetic landscape during myogenic differentiation. *Proc. Natl. Acad. Sci. U. S. A.* (2011). doi:10.1073/pnas.1102223108

89. Cao, Y. *et al.* Genome-wide MyoD Binding in Skeletal Muscle Cells: A Potential for Broad Cellular Reprogramming. *Dev. Cell* (2010). doi:10.1016/j.devcel.2010.02.014

90. Puri *et al.* Differential roles of p300 and PCAF acetyltransferases in muscle differentiation. *Mol. Cell* (1997).

91. Dilworth, F. J., Seaver, K. J., Fishburn, A. L., Htet, S. L. & Tapscott, S. J. In vitro transcription system delineates the distinct roles of the coactivators pCAF and p300 during MyoD/E47-dependent transactivation. *Proc. Natl. Acad. Sci. U. S. A.* (2004). doi:10.1073/pnas.0404192101

92. Toto, P. C., Puri, P. L. & Albini, S. SWI/SNF-directed stem cell lineage specification: dynamic composition regulates specific stages of skeletal myogenesis. *Cellular and Molecular Life Sciences* (2016). doi:10.1007/s00018-016-2273-3

93. Forcales, S. V. *et al.* Signal-dependent incorporation of MyoD-BAF60c into Brg1-based SWI/SNF chromatin-

remodelling complex. *EMBO J.* **31**, 301–316 (2012).

94. Rampalli, S. *et al.* p38 MAPK signaling regulates recruitment of Ash2L-containing methyltransferase complexes to specific genes during differentiation. *Nat. Struct. Mol. Biol.* (2007). doi:10.1038/nsmb1316

95. Palacios, D. *et al.* TNF/p38α/polycomb signaling to Pax7 locus in satellite cells links inflammation to the epigenetic control of muscle regeneration. *Cell Stem Cell* (2010). doi:10.1016/j.stem.2010.08.013

96. Verhaart, I. E. C. & Aartsma-Rus, A. Therapeutic developments for Duchenne muscular dystrophy. *Nat. Rev. Neurol.* **15**, 373–386 (2019).

97. Hoffman, E. P., Brown, R. H. & Kunkel, L. M. Dystrophin: The protein product of the duchenne muscular dystrophy locus. *Cell* (1987). doi:10.1016/0092-8674(87)90579-4

98. Emery, A. E. The muscular dystrophies. *Lancet* **359**, 687–695 (2002).

99. Petrof, B. J., Shrager, J. B., Stedman, H. H., Kelly, A. M. & Sweeney, H. L. Dystrophin protects the sarcolemma from stresses developed during muscle contraction. *Proc. Natl. Acad. Sci. U. S. A.* (1993). doi:10.1073/pnas.90.8.3710

100. Sandoná, M., Consalvi, S., Tucciarone, L., Puri, P. L. & Saccone, V. HDAC inhibitors for muscular dystrophies: progress and prospects. *Expert Opin. Orphan Drugs* **4**, 125–127 (2016).

101. Mozzetta, C. *et al.* Fibroadipogenic progenitors mediate the ability of HDAC inhibitors to promote regeneration in dystrophic muscles of young, but not old Mdx mice. *EMBO Mol. Med.* (2013). doi:10.1002/emmm.201202096

102. Aartsma-Rus, A. *et al.* Theoretic applicability of antisense-mediated exon skipping for Duchenne muscular dystrophy mutations. *Human Mutation* (2009). doi:10.1002/humu.20918

103. Iezzi, S. *et al.* Deacetylase inhibitors increase muscle cell size by promoting myoblast recruitment and fusion through induction of follistatin. *Dev. Cell* (2004). doi:10.1016/S1534-5807(04)00107-8

104. Minetti, G. C. *et al.* Functional and morphological recovery of dystrophic muscles in mice treated with deacetylase inhibitors. *Nat. Med.* **12**, 1147–1150 (2006).

105. Consalvi, S. *et al.* Preclinical Studies in the mdx Mouse Model of Duchenne Muscular Dystrophy with the Histone Deacetylase Inhibitor Givinostat. *Mol. Med.* **19**, 79–87 (2013).

106. Bettica, P. *et al.* Histological effects of givinostat in boys with Duchenne muscular dystrophy. *Neuromuscul. Disord.* (2016). doi:10.1016/j.nmd.2016.07.002

107. Segalés, J., Perdiguero, E. & Muñoz-Cánoves, P. Epigenetic control of adult skeletal muscle stem cell functions. *FEBS J.* (2015). doi:10.1111/febs.13065

108. Elaut, G., Rogiers, V. & Vanhaecke, T. The Pharmaceutical Potential of Histone Deacetylase Inhibitors. *Curr. Pharm. Des.* (2007). doi:10.2174/138161207781663064

109. Colussi, C. *et al.* Nitric oxide deficiency determines global chromatin changes in Duchenne muscular dystrophy. *FASEB J.* (2009). doi:10.1096/fj.08-115618

110. Colussi, C. *et al.* HDAC2 blockade by nitric oxide and histone deacetylase inhibitors reveals a common target in Duchenne muscular dystrophy treatment. *Proc. Natl. Acad.*

Sci. U. S. A. (2008). doi:10.1073/pnas.0805514105

111. Lee, S.-J. REGULATION OF MUSCLE MASS BY MYOSTATIN. *Annu. Rev. Cell Dev. Biol.* (2004). doi:10.1146/annurev.cellbio.20.012103.135836

112. Cacchiarelli, D. *et al.* MicroRNAs involved in molecular circuitries relevant for the duchenne muscular dystrophy pathogenesis are controlled by the dystrophin/nNOS pathway. *Cell Metab.* (2010). doi:10.1016/j.cmet.2010.07.008

113. Horak, M., Novak, J. & Bienertova-Vasku, J. Muscle-specific microRNAs in skeletal muscle development. *Developmental Biology* (2016). doi:10.1016/j.ydbio.2015.12.013

114. Xu, W. S., Parmigiani, R. B. & Marks, P. A. Histone deacetylase inhibitors: Molecular mechanisms of action. *Oncogene* (2007). doi:10.1038/sj.onc.1210620

115. Yoshida, M., Kijima, M., Akita, M. & Beppu, T. Potent and specific inhibition of mammalian histone deacetylase both in vivo and in vitro by trichostatin A. *J. Biol. Chem.* (1990).

116. Kim, H. J. & Bae, S. C. Histone deacetylase inhibitors: Molecular mechanisms of action and clinical trials as anti-cancer drugs. *American Journal of Translational Research* (2011).

117. Iezzi, S., Cossu, G., Nervi, C., Sartorelli, V. & Puri, P. L. Stage-specific modulation of skeletal myogenesis by inhibitors of nuclear deacetylases. *Proc. Natl. Acad. Sci. U. S. A.* (2002). doi:10.1073/pnas.112218599

118. Consalvi, S. *et al.* Histone Deacetylase Inhibitors in the Treatment of Muscular Dystrophies: Epigenetic Drugs for Genetic Diseases. *Mol. Med.* **17**, 457–465 (2011).

119. Birnkrant, D. J. *et al.* Diagnosis and management of Duchenne muscular dystrophy, part 1: diagnosis, and neuromuscular, rehabilitation, endocrine, and gastrointestinal and nutritional management. *The Lancet Neurology* (2018). doi:10.1016/S1474-4422(18)30024-3

120. L., L. *et al.* DNA damage signaling mediates the functional antagonism between replicative senescence and terminal muscle differentiation. *Genes Dev.* **31**, 648–659 (2017).

7 List of Publications

Sandonà M*, Consalvi S*, **Tucciarone L**, De Bardi M, Scimeca M, Angelini D, Buffa V, D'Amico A, Bertini E, Bouché M, Bongiovanni A, Puri P L*, and Saccone V*. Currently in review in Science Advances.

M. Sandoná, S. Consalvi, **L. Tucciarone**, P. L. Puri, V. Saccone, HDAC inhibitors for muscular dystrophies: progress and prospects, *Expert Opin. Orphan Drugs* **4**, 125–127 (2016). "HDAC inhibitors Modulate microRNA Content of Fibroadipogenic Progenitor-derived Exosome to Promote Regeneration and Inhibit Fibrosis of Dystrophic Muscles".

L. Tucciarone, U. Etxaniz, M. Sandoná, S. Consalvi, P. L. Puri, V. Saccone, *Advanced methods to study the cross talk between fibro-adipogenic progenitors and muscle stem cells* (2018).

S. Consalvi*, **L. Tucciarone***, M. Picozza, M. De Bardi, P.L. Puri. Epigenetic and Transcriptomic profiling of Fibro Adipogenic Progenitors during Duchenne Muscular Dystrophy progression and Histoe Deacetylase Inhibitors treatment. Manuscript in preparation.

Con il tempo capisci che utilizzare un tuo traguardo per ringraziare le persone che ami per supportarti durante il tuo cammino non ha poi molto valore.

È facile. È scontato.

Con il tempo realizzi che è molto meno scontato ringraziarle tutti i giorni regalandole un piccolo gesto, come un sorriso, per farle sentire il tuo calore. Per far sentire che ci sei e che gli sei vicino.
E questo è quello che sto provando goffamente a fare nella mia quotidianità. A volte riesce bene, a volte un po' meno, ma non per questo smetterò di provare.

Non voglio neanche fare nomi. Tu lo senti che è per te.

All'arrivo di un importante traguardo è invece utile ringraziare e gratificare l'unica persona che per tanto tempo ho trascurato: me.

Lo consiglio anche a te. Ogni tanto fermati a pensare a quanto hai fatto e trova un momento di pace per sentirti soddisfatto del tuo cammino. Se non sai dove andare non preoccuparti, troverai la tua via. Non avere paura della fine.

In questo mondo non esiste una fine.

Solo nuovi inizi.